FREQUENCY ANALYSIS OF CATHETER SYSTEMS USED FOR INVASIVE BLOOD PRESSURE MONITORING

by

Daniel Michael Chernoff

SUBMITTED IN PARTIAL FULFILLMENT OF THE REQUIREMENTS FOR THE DEGREES OF

BACHELOR OF SCIENCE

and

MASTER OF SCIENCE

at the

MASSACHUSETTS INSTITUTE OF TECHNOLOGY

June, 1982

Signature of Author.....
Department of Electrical Engineering and Computer Science, June, 1982.

Certified by.....
Roger G. Mark, M.D., Ph.D. Thesis Supervisor-Academ

Certified by.....
David M. Ellis, Thesis Supervisor (Cooperating Compa

Accepted by.....
Arthur C. Smith, Chairman
Departmental Committee on Graduate Students

ACKNOWLEDGEMENT

I am grateful for the guidance, support and surplus of enthusiasm which Mr. David Ellis supplied during the research and writing of this thesis. His help and criticisms were truly invaluable. Dr. Roger Mark provided perspective on the problem and aided in directing the focus of the research. I wish to thank the many people at Hewlett-Packard's Waltham Division who supplied ideas and moral support throughout this project.

TABLE OF CONTENTS

FREQUENCY ANALYSIS OF CATHETER SYSTEMS USED FOR INVASIVE BLOOD PRESSURE MONITORING

by

Daniel Michael Chernoff

Submitted to the Department of Electrical Engineering and Computer Science on May 1, 1982 in partial fulfillment of the requirements for the Degrees of Bachelor of Science and Master of Science in Electrical Engineering.

ABSTRACT

The resonant behavior of fluid-filled catheter manometers can produce severe distortion in the monitored blood pressure waveform. Although gradual improvements in components has resulted in catheter systems having adequate frequency response for human blood pressure measurement, these systems are frequently compromised by the presence of occult air bubbles in the fluid column.

A general model was developed to predict the frequency response of catheter systems in terms of a limited number of lumped second-order sections. This model was experimentally verified by direct frequency response measurement and by independent measurement of component characteristics. This model also successfully predicts the effect of bubble size and location on the frequency response.

A previously-proposed technique of measuring the frequency response of a fluid-filled catheter system in vivo was described and theoretically justified in terms of the lumped element system model. This technique is believed to have significant clinical application in dynamic in situ testing of catheter systems. Utilization of this technique may result in higher user confidence in the catheter system.

Thesis Supervisor: Dr. Roger G. Mark, M.D., Ph.D.

Title: Matsushita Associate Professor of Electrical Engineering in Medicine

LIST OF TABLES

LIST OF FIGURES

CHAPTER 1

INTRODUCTION

Present-day invasive pressure monitoring is typically accomplished using a fluid-filled catheter leading from the measurement site to an externally located transducer. This measurement system has nonideal frequency response characteristics, often represented as second-order, with the existence of one or more resonant peaks and nonlinear phase shift. With properly assembled modern equipment, the resonance will usually occur at a frequency well beyond the highest frequency components of the pressure signal, permitting simple low-pass filtering to yield satisfactory waveform reproduction while suppressing high-frequency artifact. However, a number of factors, most often trapped air in the fluid line, contribute to a low resonant frequency and subsequent distortion of the waveform that cannot be corrected by low-pass filtering. This distortion may have serious consequences, since various features of the waveform are used in clinical diagnosis. Measurement of satisfactory frequency response before catheter insertion can lead to the erroneous and even dangerous assumption that the frequency response remains satisfactory while the system is in use. There is strong evidence to suggest that dynamic changes in the system - clotting at the catheter tip, movement and coalescence of microbubbles, etc. - can seriously alter the frequency response.

The primary objective of this study is to examine techniques of determining the approximate frequency response of a catheter system in vivo (while attached to the patient). We will examine two direct time-domain techniques for doing-this:

(1) The fast-flush technique proposed by Gardner (1970);

(2) A flow impulse produced by tapping the catheter or extension tubing.

We will compare these two excitations with a method (pressure step at the catheter tip) that cannot be performed in vivo but is an established technique for measuring frequency response.

Because the theoretical model we choose to represent the system has a considerable influence on our interpretation of the above stimuli, the other major objective of this study will be to examine transmission-line and lumped-element models of the catheter system. Using independent evidence, we will determine which model is the more accurate representation and how the two models may be reconciled. This analysis will aid considerably in our understanding of how bubble size and position affect the frequency response of the system and the time response to the proposed excitations.

1.1 Brief History of Invasive Monitoring

Invasive blood pressure monitoring of the critical-care and post-surgical patient has become almost commonplace in modern medical practice. The visual display of the blood pressure

waveform often yields to the clinician valuable information on the dynamic state of the cardiovascular system. The ability to monitor pressure at a number of important sites in the vasculature, such as in the great vessels and chambers of the heart, is often an invaluable diagnostic tool. Long-term monitoring has led to the incorporation of high- and low-pressure alarms into monitoring systems, resulting in faster response of hospital personnel to potentially life-threatening conditions.

There are at present two methods in common use for invasive blood pressure monitoring. The catheter-tip manometer is a relatively new device, prompted by advances in microelectronics and semiconductor technology, which consists of a very small strain-gauge transducer located on the tip of a catheter. These manometers have excellent frequency response characteristics, but suffer the disadvantages of high-cost, extreme fragility, and high temperature sensitivity. The older and more common method consists of an external strain-gauge transducer coupled to the recording site via a hollow fluid-filled catheter, first reported in its modern form by Lambert and Wood (1947). The catheter is generally constructed of polyethylene, PVC, woven dacron, or nylon, and is filled with a saline solution. This recording system, while having a significant cost advantage over the catheter-tip manometer, suffers from relatively poor frequency response, which at times makes it inadequate for high-fidelity measurement of the blood pressure waveform.

1.2 Requirements for Accurate Waveform Reproduction

A number of studies have been published which recommend a certain minimum bandwidth for faithful reproduction of the blood pressure waveform. Geddes (1970) provides a summary of these reports, in which it is apparent that "adequate frequency response" depends both on the nature of the waveform and the degree of accuracy required, neither of which has been standardized. Bruner (1981) has correctly observed that there is still little consensus on the minimum frequency requirements of these systems, and he offers an excellent analysis of the practical difficulties which have prevented such a consensus from being reached. The pressure waveform has also been subjected to fourier analysis to determine the number of harmonics neccessary to achieve a certain fidelity in a reconstructed waveform. These analyses all show the magnitude of the fourier components dropping off rapidly with the harmonic number: Hansen (1949) showed that the amplitude of the components of an arterial waveform had fallen to 11.8% by the sixth harmonic; McDonald (1960) found the amplitude of the fifth harmonic from a number of pressure recordings to be less than 20% of the fundamental. These findings tend to support the view that the higher harmonics do not contribute significantly to the arterial pressure wave, but it should be stressed that reconstruction of a wave from a limited number of harmonics is not equivalent to passing it through a distorting measurement system, since the underdamped nature of the system causes nonlinear gain and phase shift within the passband.

None of these studies directly analyzed the effect of an underdamped second-order system on the pressure waveform. Gardner (1981) has done this, specifying an approximate range, in the form of a chart, of resonant frequencies and damping coefficients which yield acceptable reproduction of "demanding" pressure waveforms. This represents a practical if incomplete effort at defining an acceptable frequency response in terms of preserving the important features of a waveform (particularly systolic and diastolic values). This type of analysis is clearly needed, along with a clear definition of the waveform features to be preserved, if an objective evaluation of the adequacy of a given transducing system with known frequency response is to be made.

1.3 The Fluid-Filled Catheter

1.3.1 Models

The mechanical properties of fluid-filled catheter systems which lead to inadequate frequency response have undergone a great deal of study. Hansen and Warburg (1949) modeled the system as a harmonic oscillator (system with one degree of freedom), generally extending the work of Frank (1903). The coefficients of the second-order equation governing the frequency response of this model could be shown to be related to the compliance of the elements of the system, the physical dimensions of the catheter, and the mass of fluid filling the system. This is analogous to a mechanical lumped-element system consisting of a mass, spring, and dashpot in series, or an electrical system composed of an

inductance, capacitance, and resistance.

This early work in modeling was extended by the experimental work of a number of researchers. These include Yanof et al (1963), Shapiro and Krovetz (1970), Falsetti et al (1974), Krovetz et al (1974), Fox et al (1978), and Shinozaki et al (1980), who evaluated the frequency response in more detail but retained the second-order system as the fundamental model for their analysis. Another group of workers, including Vierhout (1966), Latimer (1968), and Li et al (1978), started from the basic equations of fluid flow in tubes, derived originally to study pulse wave transmission in the arterial system, and developed a transmission line model for the catheter system. This model has been shown to be more accurate than the simple second-order model in determining the location of the first resonant frequency from the physical constants of the system and in predicting the presence of higher order resonances. However, since the primary goal of many workers has been to fit the observed frequency response in the lower frequency range with a model, and not to determine the response a priori, the second-order system has been the more commonly cited model.

1.3.2 Distortion

An ideal pressure measurement system is one which has flat frequency response to well beyond the highest harmonic of interest, and either zero or linear phase shift (linear phase shift corresponds to a pure time delay). This guarantees an output which is at worst a time-delayed but otherwise undistorted

version of the input. The physical laws governing pressure transmission in a long flexible fluid column make this extremely difficult to achieve.

The magnitude and phase response of a typical catheter system is shown in Figure 1-1. There is present a large resonant peak which will amplify harmonics that lie close to the resonance, and a subsequent falling off of the frequency response following the resonance which will attenuate higher harmonics. Moreover, the phase shift is highly nonlinear, with a sudden 180 degree phase shift near the resonant frequency. This type of frequency response is typical of underdamped second-order systems.

Figure 1-2 illustrates the effect this type of distortion has on a simulated arterial pressure waveform. Figure 1-2(a) shows the input to the catheter, while Figure 1-2(b) shows the output from tne system. The output signal exhibits serious distortion resulting from the nonideal characteristics of the recording system, particularly the appearance of spurious oscillations and large error in systolic pressure.

While it is theoretically possible to recover the input signal given the output waveform and the frequency response of the system, the latter is generally unknown. Therefore, a great deal of work has gone into measuring the frequency response of catheter systems, either to perform this reconstruction or simply to evaluate the adequacy of the system.

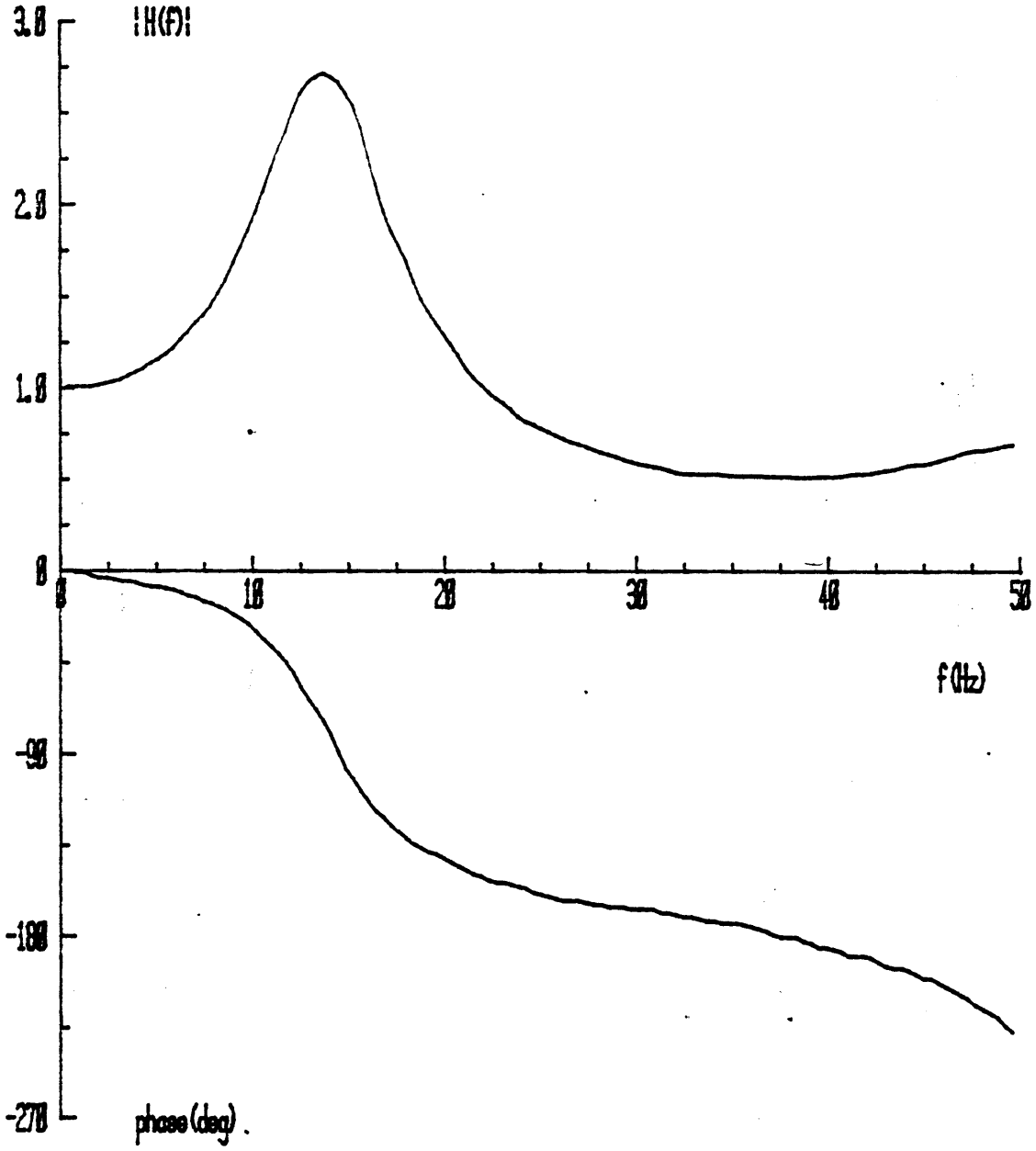

Figure 1-1. Magnitude and phase response of a typical catheter system

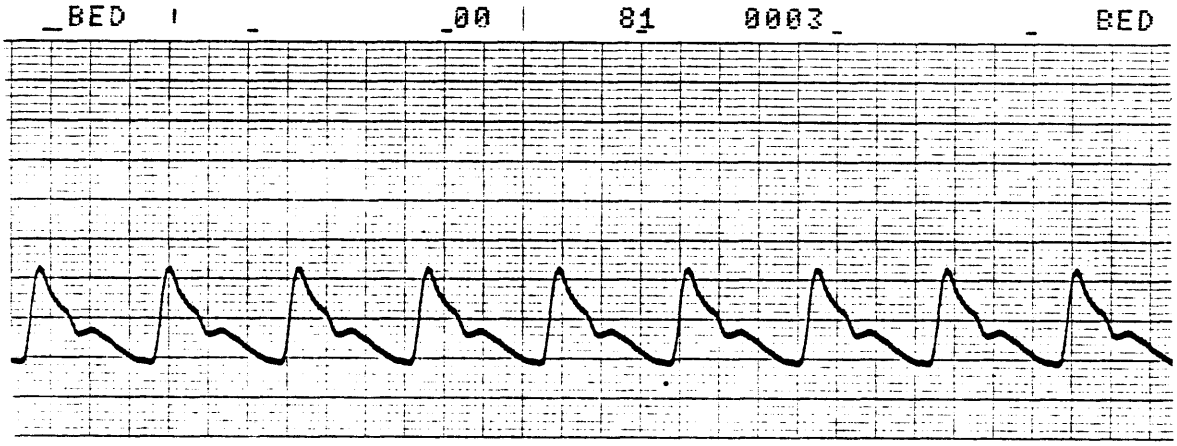

input blood pressure waveform
(a)

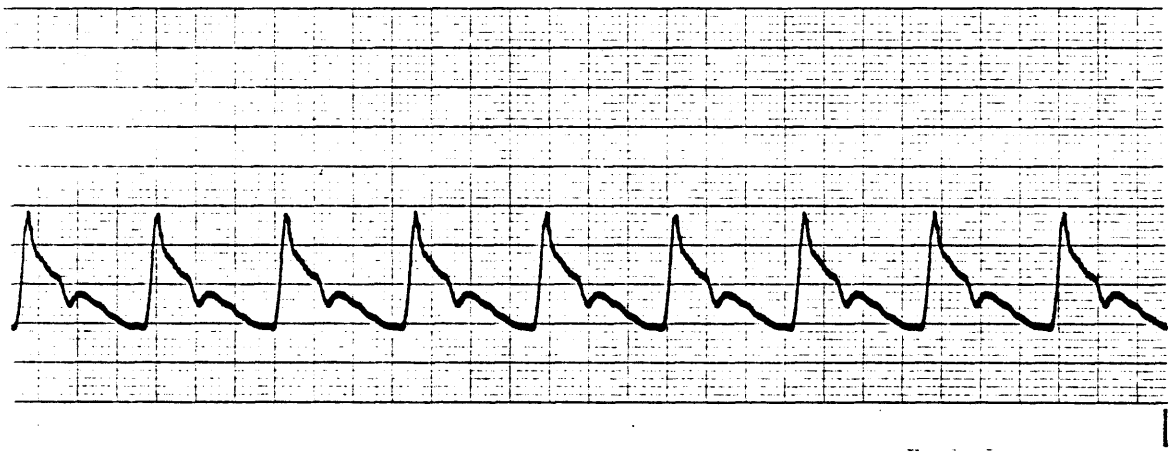

output of catheter-transducer system
(b)

Figure 1-2. Waveform distortion due to nonideal frequency response

1.4 Frequency Response Measurement Techniques

A number of techniques have been used to deduce the frequency response of catheter systems. These techniques can be separated into two classes: (1) direct techniques, which involve analyzing the system response to a known external input; and (2) indirect techniques, which assume a particular model for the catheter (typically second-order) and make additional assumptions about the frequency content of the input signal. Within each class, the techniques can be further divided into time, frequency, and correlation-domain approaches. We will examine how each of these techniques has been used.

1.4.1 Direct Techniques

Frequency-domain techniques all require input of a signal having a known spectrum. If the system is linear and time-invariant, the energy at each frequency in the output signal is uniquely associated with the energy in the input signal at that frequency, so an input which is flat in frequency and phase will produce an output which is a scaled version of the transfer function. The impulse function and white noise both are flat in frequency and phase, but practical considerations make white noise the better choice for frequency-domain measurement. There is no evidence of white-noise excitation having been used for direct frequency-response measurement in catheter systems, possibly because other methods exist which do not require the data to be analyzed directly in the frequency domain, therefore requiring less sophisticated instrumentation.

An example of one such alternate method is to measure the gain and phase shift at a number of discrete frequencies. This technique was used quite successfully by Latimer and Latimer (1968). Swept frequency measurement is a standard engineering technique which has been recently been used by Rothe and Kim (1980), and Gardner (1981). Unfortunately, all of the measurements described thus far require that the system be removed from the patient and an appropriately driven pressure source substituted for the artery at the catheter tip. This requirement is difficult to meet in the clinical environment. Therefore it is not surprising that these methods have primarily been used in experimental work.

Direct time-domain techniques for measuring the frequency response all consist of exciting the system with a simple well-described time signal, usually a step function of pressure ("pop" excitation). The pressure step is achieved by pressurizing a closed system and then suddenly relieving the pressure at the catheter tip, typically by bursting a rubber membrane. The response observed at the output of the system can then be analyzed. In order to make the analysis of the response waveform straightforward, the system order is generally described a priori. While most researchers have assumed a second-order system, some (Melbin and Spohr, 1969; Gabe, 1972; Krovetz et al, 1974) have demonstrated systems which exhibit higher-order responses to the pressure step, although only Krovetz specifically suggests that reflections from impedance mismatches (i.e. transmission-line phenomena) may be responsible. One source

(Attinger, 1969) reports that 30% of a large number of systems tested exhibited higher than second-order behavior. However, the second-order approximation is often satisfactory, and this assumption makes the waveform analysis particularly simple (see Appendix A).

Even if a satisfactory model for the system is chosen, the "pop" technique remains unsuitable for dynamic analysis of the catheter in vivo, since it requires that the catheter tip be available. Because catheter systems can collect bubbles, become clotted, or otherwise be degraded in use, a satisfactory test result from a pop test performed prior to insertion may give a false sense of security. This concern raises the question of whether excitations applied elsewhere in the system may elicit a response from which the appropriate transfer function may be deduced. There have been no studies done to answer this question, although Gardner (1981) has described a technique which is claimed to be an acceptable excitation: a flow step created by opening and then releasing the flush valve present in most monitoring setups, where the flush source is located at the transducer end of the fluid column.

1.4.2 Indirect Techniques

A number of indirect distortion-measuring techniques have been described. These all assume a second-order model and attempt to determine, from the patient pressure signal itself, the location and magnitude of the resonance. Brower et al (1975) examined the magnitude of the signal spectrum after

preconditioning (bandpass filtering and differentiation). The presence of a peak in the preconditioned spectra was associated with distortion, and approximate formulae given for determining the degree of damping. Doherty (1981) determined the Fourier components of the incoming pressure signal, and applied the normalized magnitude and phase in a regression equation whose coefficients were optimized to detect resonance within a certain critical range. Jackson et al (1978) used linear predictive analysis (a correlation technique) to model the spectrum of the input signal: the presence of a complex pole pair within a certain range of frequencies was taken to indicate the presence of resonance. .

These indirect techniques all evolved because of the need to perform dynamic analysis on the catheter system and to eliminate the need for manual intervention by hospital personnel, either in testing the system or in compensating the response. These advantages over direct methods make indirect techniques extremely desirable. On the other hand, the validity of these indirect techniques rely heavily on both the assumed catheter system model and on the assumed spectrum of the patient waveform. If the blood pressure power spectrum appears "resonant" in the sense of having a local maximum, as may happen in recordings from the smaller arteries (the arterial system itself behaves as an assemblage of branched transmission lines), then these techniques can give erroneous results. An additional problem, although one that has grown smaller as the cost of computation has decreased, is the computational complexity of indirect analysis. Although initial

experiments using these techniques appear promising, they have not yet been subjected to extensive testing using the full range of clinically observed waveforms.

1.5 Compensation Techniques

Various approaches have been taken to compensate the frequency response of catheter systems. These can be divided into two classes, mechanical and electrical. Mechanical compensation may be considered a problem in impedance matching, although some researchers regard it as merely increasing the damping coefficient. Electrical compensation involves active filtering of the signal. We will now examine each of these methods in more detail.

1.5.1 Mechanical Compensation

By adding additional damping to the hydraulics, a catheter system which previously produced highly distorted waveforms can be made to have a much wider useful bandwidth. Damping by adding a constriction at the patient end of the catheter has been used for many years. A set of experiments by LaPointe and Roberge (1974), using needle valves as resistance elements, has confirmed the utility of the technique, and Latimer (1968) has justified it in terms of matching the source and line impedance of an acoustic transmission line. Unfortunately, the large amount of constriction neccessary to achieve appreciable damping makes this technique unsuitable for use with flush devices, and it is rather sensitive as well. A more promising technique is parallel

damping, reported by van der Tweel (1957) and Crul (1962). This can be described as another form of impedance matching, this time matching the load (transducer) impedance to the line impedance. There are commercial devices now available to perform parallel damping. One which we have observed is the Sorenson Accunamic, which is placed in parallel with the fluid line at the transducer. Gardner (1981) has described this device, in which a fixed compliance (bubble) is placed in series with a variable resistance (needle valve) in order to create an adjustable parallel impedance. The impedance match obtained by empirically adjusting this device to minimize step response overshoot is crude but nonetheless fairly effective.

An advantage of these mechanical compensation techniques is that, by effectively increasing the damping to flatten out the resonant peak, they tend to extend the useful range of the system out to approximately the resonant frequency. This can amount to twice the usable bandwidth of the uncompensated system. Moreover, no exotic electronics or processing techniques are required. The chief disadvantage of mechanical compensation is that it requires an external step input to observe when critical damping is achieved. Relying on the patient waveform to adjust the damping is a dubious procedure at best.

1.5.2 Electrical Compensation

If an approximate transfer function for the catheter system is known, inverse filtering (convolving the output signal with a network having the inverse transfer function) can greatly extend

the bandwidth. Melbin and Spohr (1969) describe an analog circuit to perform inverse filtering. More recently, Brower et al (1975) and Ciccolella (1976) have described digital filtering to perform the same function.

If the transfer function is not known, the most common approach is to low-pass filter the signal, with a cut-off frequency lower than the assumed resonance but high enough to retain the significant harmonics of the pressure signal. This is the method most manufacturers include in the monitors at present. Frequently, however, these conditions cannot be met simultaneously - the resonant peak overlaps an appreciable portion of the signal spectrum. Aggressive low-pass filtering (12 Hz cutoff and below) has been practiced by some manufacturers in an attempt to prevent resonances occuring at higher frequencies from causing systolic overshoot, but at the cost of extremely limited bandwidth. Low-pass filtering can be useful in preventing high-frequency artifact from appearing in the output signal, but it is extremely limited in its ability to compensate systems having low resonant frequencies.

CHAPTER 2

MODELING OF THE CATHETER SYSTEM

A theoretical understanding of the blood pressure transducing system is an important step towards being able to predict the changes in system characteristics under various conditions (e.g. altering of component stiffness, tubing length, the presence of occult bubbles or leaks). Under an appropriate system model, it is possible to specify the most desirable characteristics for catheter, tubing, and transducer in terms of producing a faithful reproduction of the pressure waveform. In addition, an accurate model for the system may suggest methods of compensation of the frequency response involving additional components, such as impedance matching devices. This section will develop a general model for the transducing system using the well-established theory of wave propagation in transmission lines, and then proceed to establish conditions under which the model may be simplified to a lower order lumped-parameter system with little loss in accuracy and large gain in ease of analysis.

2.1 General Model - Mechanical/Electrical Analogies

There can be little doubt as to the validity of a transmission line model for the fluid-filled pressure tubing. The presence of phase delay, attenuation, and acoustic impedance have

been experimentally demonstrated by many researchers, but perhaps most elegantly by Latimer and Latimer (1969), who determined values for wave speed and attenuation at a number of resonant and antiresonant frequencies. It is interesting to note that the theory of acoustic wave transmission in elastic tubes was originally developed not for catheter systems but rather for pulse wave transmission in the arterial tree. The principles are largely the same but the catheter system is in fact easier to analyze due to the limited number of reflecting sites, consistent internal diameters and better-understood wall properties.

Figure 2-1(a) shows a physical model for the simplest type of transducer system, represented by a liquid-filled tube of constant internal diameter coupled to a transducer through a fluid-filled dome. An increase in pressure initiated at the left causes liquid to flow to the right through the tubing and dome, which in turn causes a deflection of the transducer diaphragm. This deflection is sensed by a strain gauge and the resulting electrical signal is amplified and processed to produce a pressure recording.

An electrical model for this mechanical system is shown in Figure 2-1(b). The tubing and transducer dome/diaphragm will each be examined in turn. In each infinitesimally long segment of the tubing, fluid motion has associated with it friction due to shear stresses in the fluid and inertia due to the mass and velocity of the fluid. There are also compliances associated with the tubing wall and (to a lesser extent) in the fluid itself, leading to storage of potential energy. Finally, the wall exhibits

viscoelasticity which causes energy losses due to mechanical hysteresis effects. These physical "line constants" are replaced by the analogous electrical symbols in Figure 2-1(b), where:

R' = resistance/unit length due to viscosity of the fluid;

L' = inertance/unit length due to the mass of the fluid;

C' = compliance/unit length due to compressibility of the fluid and stretch of the tube walls;

G' = conductance/unit length due to energy loss in the tube walls;

dx = incremental length.

These so-called "line constants" are in fact all frequency dependent to some extent as the theoretical development of the next section will show. The transducer dome and diaphragm also exhibit similar resistive, inertial, wall loss, and elastic effects, but the short length of the transducer relative to the wavelengths we will be considering justifies treating these as lumped elements.

In summary, then, we have inertial and resistive effects associated with the fluid. These present a longitudinal impedance to flow and thus are represented as series elements. The compliance and wall loss are properties of the plastic materials used, present a transverse impedance to flow, and thus are represented as parallel elements. An infinite sum of these infinitesimal sections then produces a transmission line characterized by the telegraph equations of electrical engineering theory. Prior to determining the frequency response of this model, however, we will need to develop the equations to calculate values for the line constants.

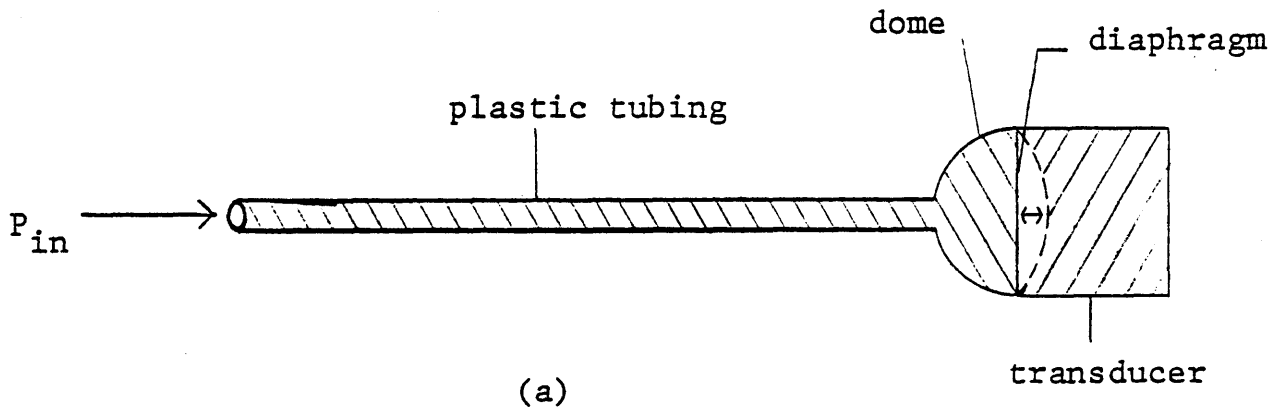

(a)

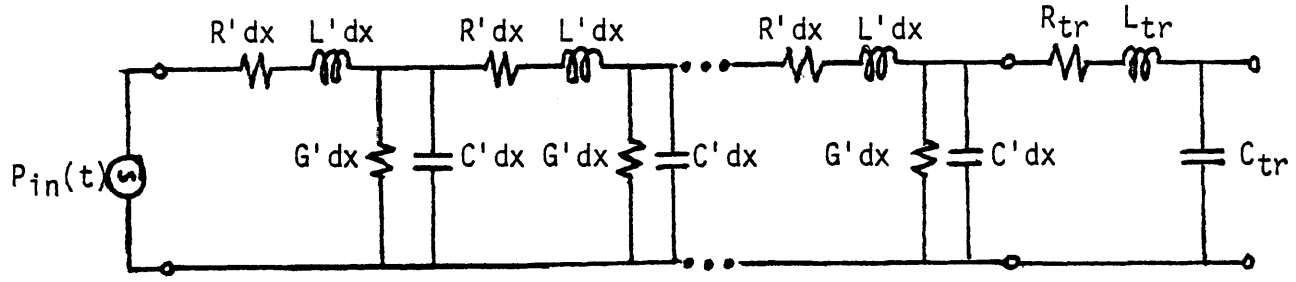

(b)

Figure 2-1. Modeling the catheter system

2.2 Theoretical Calculation of Line Constants

2.2.1 Longitudinal Impedance (R and L)

The development of theory describing laminar oscillatory fluid flow through narrow tubes has been made by Lambossy (1956) and Womersley (1956). The most significant result of this theory is the prediction of a "skin effect" phenomenon, which causes an increase in resistance and decrease in inertance at high frequency due to alteration of the fluid velocity profile across the tubing cross-section. If the tubing is assumed to be rigid, straight, and of circular cross-section Womersley shows that

$$Q = \pi r^2 \frac{A}{j\omega\rho}\left[1 - \frac{2J_1\{\sigma j^{3/2}\}}{\sigma j^{3/2} J_0\{\sigma j^{3/2}\}}\right] e^{j\omega t} \qquad (1)$$

where

Q = volume flow

A = amplitude

ω = circular frequency = $2\pi f$

$Ae^{j\omega t}$ = pressure gradient = $-dp/dx$

ρ = fluid density

$\sigma = r\sqrt{\omega/\upsilon}$ = Womersley coefficient (dimensionless)

$\upsilon = \mu/\rho$ = kinematic viscosity

J_0 and J_1 are the zero and first-order Bessel functions of the complex argument

$\sigma j^{3/2}$; $j = \sqrt{-1}$ = phase shift of $\pi/4$ radians

Although the requirements of rigid and straight tubing are

not strictly met by catheter systems, many authors (Latimer, Jager) have applied these equations to calculate the longitudinal impedance per unit length Z'_ℓ with good results. Following the analysis of Jager et al (1965):

$$Z'_\ell = \frac{dp/dx}{Q} = \frac{j\mu}{\pi r^4}\left[1 - \frac{2J_1\{\sigma j^{3/2}\}}{\sigma j^{3/2} J_0\{\sigma j^{3/2}\}}\right]^{-1} \qquad (2a)$$

if we write this as

$$Z'_\ell = j\,L'(\omega) + R'(\omega) \qquad (2b)$$

where L' and R' denote resistance/unit length and inertance/unit length, respectively, then

$$L'(\omega) = \frac{\rho}{\pi r^2 M'_{i0}\sigma^2}\cos\varepsilon'_{i0} \quad ; \quad R'(\omega) = \frac{\mu}{\pi r^4 M'_{i0}}\sin\varepsilon'_{i0} \qquad (3a,b)$$

$$M'_{i0} = \text{modulus}\left\{1 - \frac{2J_1}{\sigma j^{3/2} J_0}\right\}; \quad \varepsilon'_{i0} = \text{phase}\left\{1 - \frac{2J_1}{\sigma j^{3/2} J_0}\right\}$$

For the case of steady flow these equations reduce to the familiar Poiseuille equations for R' and L':

$$R'_w = \frac{8\mu}{\pi r^4} \quad ; \quad L'_w = 4/3\,\frac{\rho}{\pi r^2} \qquad (4)$$

The significance of the Womersley calculations for R' and L' is that as the frequency of oscillation is increased, the effective inertance decreases and the effective resistance increases. In the limit of infinite frequency, the inertance drops to 75% of its d.c. value, and the resistance becomes

infinite. A plot of $R'(\omega)$ and $L'(\omega)$ vs. ω for the tubing dimensions used in this study is shown in Figure 2-2. The viscosity and density of saline have been taken as 0.01 poise and 0.998 gm/cm^3 respectively (approximate values at 20 degrees centigrade).

2.2.2 Transverse Impedance (C and G)

A calculation of compliance and wall loss requires detailed knowledge both of the physical properties of the plastic used for the pressure tubing and the mode(s) of wave propagation in the fluid and in the wall. These are generally quite difficult to specify precisely. Equations exist which specify the compliance of a tube of uniform cross-section as a function of the internal and external radii, Young's modulus and the Poisson ratio for the tubing material. These assume a linear, isotropic medium with no losses, but may be applied to plastics so long as the results are not expected to be quantitatively precise. Using the equation for the compliance of a thick-walled tube (see reference 25) we have:

$$C' = \frac{2\pi r_i}{E} \frac{1+r_i^2/r_e^2}{1-r_i^2/r_e^2} + s \qquad (5)$$

where

r_i = internal diameter;

r_e = external diameter;

E = Young's modulus;

s = Poisson's ratio.

No such simple equation is known describing the wall loss G, and

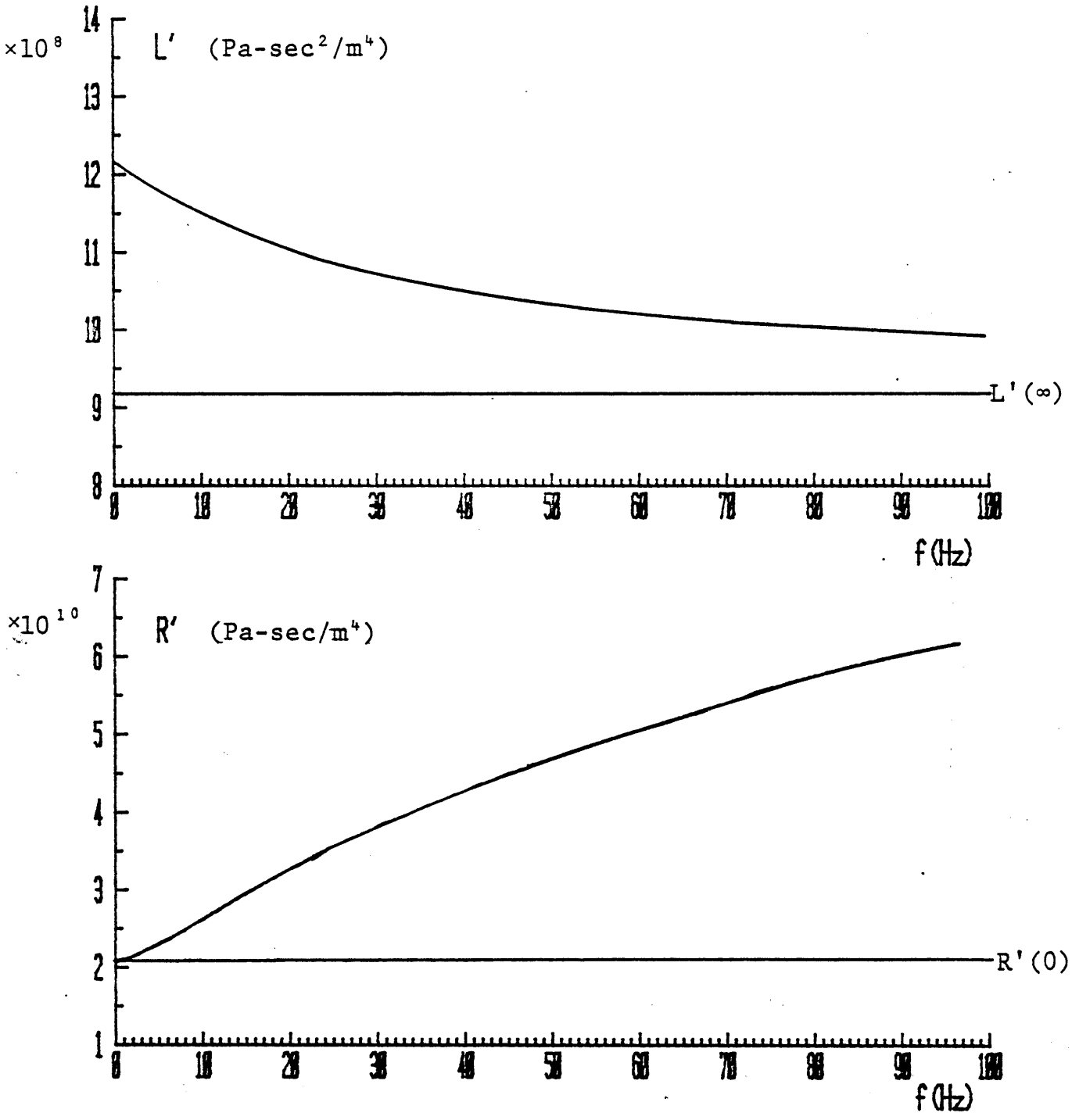

Figure 2-2. R' and L' as a function of frequency

in any case the properties of a given sample of plastic are generally not so well specified as to allow direct calculation of compliance and wall loss. In other studies similar to this one, experimental measurements are invariably substituted for theory in the calculation of transverse impedance. Hansen (1949) has found that G' is proportional to frequency, implying a mechanical hysteresis loss per cycle, but it is not known whether this is generally true for plastic materials. More research in this area is clearly needed but is beyond the scope of the present study. We will use experimentally determined values for C' in our models, and assume G'=0. As long as $G'/\omega C'$ is small, this assumption should cause negligible error in predicted location of resonant frequency.

2.3 Transmission Line Formulation

2.3.1 Telegraph Equations and Propagation Constant

We will take the following circuit representation to be an adequate model of the transducing system:

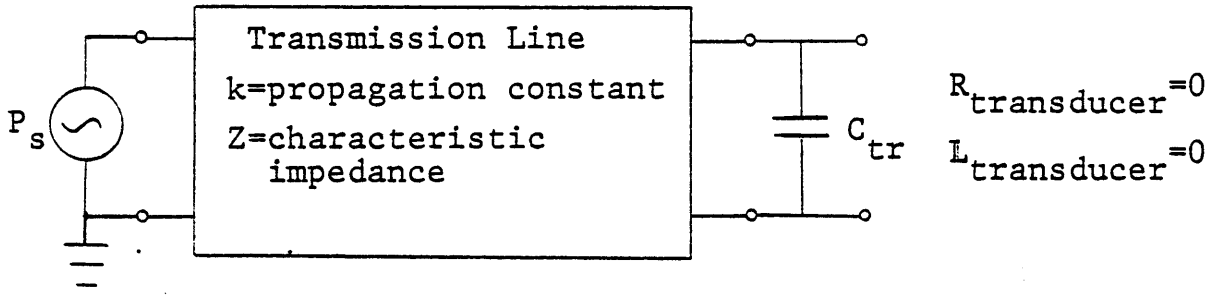

where the parameters R_{tr} and L_{tr} have been set to zero. This is justified when the transducer dome radius (or effective radius in the case of a non-cylindrical dome) is much larger than the tubing radius, due to the strong inverse dependence of both R and L on the radius. This condition is nearly always met in catheter systems. The telegraph equations governing this line are:

$$dP/dx = -(R'+j\omega L')Q \qquad (6a)$$

$$Q = -(G'+j\omega C')P \qquad (6b)$$

where P represents pressure and Q is flow. If we assume a solution which is the sum of forward and backward traveling waves:

$$P(x,t) = \{P_+ e^{-kx} + P_- e^{+kx}\} e^{j\omega t} \tag{7}$$

then we can solve for k:

$$k = \alpha + j\beta = \sqrt{(R'+j\omega L')(G'+j\omega C')}$$

$$= \omega\sqrt{L'C'}\ \sqrt{(V+j)(W+j)}$$

$$= \beta_0\sqrt{(V+j)(W+j)} \tag{8}$$

where

α = attenuation constant

β = phase constant

$\beta_0 = \omega\sqrt{L'C'}$

$V = R'/\omega L'$

$W = G'/\omega C'$

squaring the above equation:

$$k^2 = \alpha^2 - \beta^2 + 2j\alpha\beta = \beta_0^2\sqrt{(VW-1)+j(V+W)} \tag{9}$$

separating real and imaginary terms and solving, we have:

$$\alpha = 0.5F\beta_0(V+W) \tag{10}$$

$$\beta = \beta_0/F \tag{11}$$

where

$$F = \frac{2}{\sqrt{\{(1+V^2)(1+W^2)+1-VW\}}} \tag{12}$$

F is the correction factor, important primarily at very low frequencies, in the form derived by Latimer and Latimer (1968). This correction factor will rarely need to be used in this study, since by the first resonant frequency F will nearly always have reached its high-frequency limit of 1. It is, however, of theoretical interest because if the condition V = W occurs (i.e.

R'/L'=G'/C'), then F = 1 and a Heaviside "distortionless line" is obtained, with constant attenuation and phase shift proportional to frequency. This condition, unfortunately, is never encountered in practice except at isolated frequencies, because R', L', G', and C' are all frequency dependent to some extent.

2.3.2 Characteristic impedance

The characteristic impedance Z of the transmission line is defined as

$$Z = \frac{Q}{dP/dx}$$

where Q is the volume rate of flow and dP/dx the pressure differential. Z can be expressed in terms of V and W as follows:

$$Z = \sqrt{(R'+j\omega L')(G'+j\omega C')} \qquad (13)$$

$$= \sqrt{L'/C'}\sqrt{(V+j)/(W+j)} = |Z|e^{j\theta} \qquad (14)$$

$$|Z| = Z_0\{(V^2+1)/(W^2+1)\}^{.25} \qquad (15)$$

$$\theta = 0.5(\cot^{-1}V - \cot^{-1}W) \qquad (16)$$

$$Z_0 = \sqrt{L'/C'}$$

alternatively, Z may be expressed in terms of resistance and reactance:

$$Z = |Z|(\cos\theta + j\sin\theta) \qquad (17)$$

2.3.3 Boundary Conditions and Reflection Coefficient

The solution for P(x,t) and Q(x,t) can be expressed as

$$P(x) = P_+ e^{-\alpha x} e^{-j\beta x} + P_- e^{+\alpha x} e^{+j\beta x} \qquad (18a)$$

$$Q(x) = \frac{1}{Z}\{P_+ e^{-\alpha x} e^{-j\beta x} - P_- e^{+\alpha x} e^{+j\beta x}\} \qquad (18b)$$

where we have dropped the time dependence $e^{j\omega t}$ from the equations. The parameters α and β denote the attenuation per unit length and phase shift per unit length respectively of the transmission line.

To solve equation (18) we need to specify the boundary conditions at each end of the transmission line. We have assumed a zero-impedance pressure source and a load (the transducer) represented as a pure compliance. The boundary conditions are therefore

$$P(x=0) = P_+ + P_- = P_0 \qquad (19a)$$

$$Q(x=l) = j\omega C_{tr}\{P_+ e^{-kl} + P_- e^{+kl}\} = \frac{1}{Z}\{P_+ e^{-kl} - P_- e^{+kl}\} \qquad (19b)$$

Defining the reflection coefficient $\Gamma = P_+/P_-$ and solving equation (19):

$$P_+ = P_0 \frac{1}{1+\Gamma e^{-2kl}} \quad ; \quad P_- = P_0 \frac{\Gamma}{1+\Gamma e^{-2kl}}$$

and

$$P(x) = \frac{P_0}{1+\Gamma e^{-2kl}} (e^{-kx} + \Gamma e^{-2kl} e^{kx}) \qquad (20)$$

where

$$\Gamma = \frac{1-j\omega C_{tr}Z}{1+j\omega C_{tr}Z} \tag{21}$$

At the transducer, the pressure is

$$P(\ell) = \frac{P_0 e^{-k\ell}}{1+\Gamma e^{-2k\ell}} (1+\Gamma) \tag{22}$$

a relation which describes the attenuation and phase shift of the pressure wave from input to output as a function of frequency.

2.3.4 Natural Frequencies

The transmission line equations (18a,b) may also be solved for the natural resonant frequencies of the system by setting $P(x=0) = 0$. Equation (19) then becomes

$$Z \cdot \tanh k\ell = -1/j\omega C_{tr} \tag{23}$$

a transcendental equation in complex Z and k which cannot be solved in closed form. However, we can find approximate values for the natural frequencies by making the assumption $\omega >> R'/L'$ and $\omega >> G'/C'$ (generally valid at and above the first resonant frequency), allowing us to make the approximations $k \cong j\omega\sqrt{L'C'}$, $Z \cong \sqrt{L'/C'}$ in which case equation (23) becomes

$$\omega C_{tr} \sqrt{L'/C'} \tanh(\omega\ell\sqrt{L'C'}) = 1 \tag{24}$$

which can be solved graphically or numerically for the natural frequencies ω_n.

2.4 Lumped Model Approximation

While the transmission line model in theory is probably the most accurate representation of the catheter system, there are several practical reasons why lumped-parameter models are more commonly invoked to explain the resonance phenomenon. First among these is the fact that higher-order (i.e. three-quarter-wave and above) resonances almost invariably occur at a frequency beyond the range of significant blood pressure harmonics, making their presence inconsequential. A second factor tending to minimize the importance of the higher resonances is the Womersley effect, which causes the resistance (and therefore damping) to increase markedly with frequency, thus minimizing the height of the resonant peaks. Thirdly, the presence of trapped air bubbles (a common circumstance) introduces large lumped compliances into the system, tending to make a lumped circuit representation more tractable than the corresponding transmission line model.

A simple way to approximate the transmission line model with lumped-elements is to take the circuit representation of Figure 2-1(b) but let each section represent a finite length of tubing, rather than taking the limit dx->0. Li, Van Brummelen, and Noordergraaf (1978) have performed this analysis for N=1,2, and infinity, where N is the number of lumped sections. These authors also considered the effect of different element configurations (π vs. inverted-L) on the calculated frequency response. Their findings indicate that sizable errors in the location of the first resonant frequency are introduced for N=1, but that as the

length of each section becomes small relative to the shortest wavelength (highest frequency) of interest, the approximation becomes very good. They also found the π configuration, which involves slightly less lumping per section, to be more accurate for a given N than the inverted-L model.

We will adopt a slightly different tack in this study. First, we will examine the two limiting cases $C_{tu} << C_{tr}$ and $C_{tu} >> C_{tr}$, and demonstrate how each can be represented by a second-order circuit with appropriate correction factors. Then, a simple equation will be constructed which is precise for the limiting cases and introduces only a small calculable error in resonant frequency for intermediate cases where neither compliance dominates.

Ctu << Ctr

In this case the tubing is rigid compared with the transducer, and the wavespeed is so high that propagation effects may be ignored. A second-order equation is therefore valid, with

$$\omega_0 = 1/\sqrt{LC_{tr}} \qquad (25)$$

Ctu >> Ctr

In this case the transducer looks like an open circuit, and we may solve equation (24) for $C_{tr}=0$:

$$\omega_0 = \pi/2\sqrt{LC_{tu}} \qquad (26)$$

Ctu ≅ Ctr

Let us construct the following equation which will satisfy

both limiting cases:

$$\hat{\omega}_0 = \frac{1}{\sqrt{L((2/\pi)^2 C_{tu}+C_{tr})}} \tag{27a}$$

$$\hat{D} = \frac{R}{2}\sqrt{C_{eq}/L} \tag{27b}$$

where $$\hat{\omega}_r = \hat{\omega}_0\sqrt{1-D^2} \tag{27c}$$

$$C_{eq} = C_{tr} + (2/\pi)^2 C_{tu} \ .$$

For $C_{tu} << C_{tr}$:

$$\hat{\omega}_0 \rightarrow 1/\sqrt{LC_{tr}}$$

and for $C_{tu} >> C_{tr}$

$$\hat{\omega}_0 \rightarrow \frac{\pi}{2\sqrt{LC_{tu}}}$$

as desired.

We can separately solve equations (24) and (27) for intermediate values of Ctr. If we define

$$\kappa = Ctr/Ctu$$

then we can plot the relative error in predicted natural frequency $(1 - \hat{\omega}_0)/\omega_0$ as a function of κ. This is shown in Figure 2-3. The maximum error is only 2.44%, so the approximation introduced by equation (27(a)) seems acceptable. If the precise values of C_{tr} and C_{tu} are known, Figure 2-3 can be used to determine a correction factor for equation (27(a)).

Thus we have succeeded in reducing the transmission line to

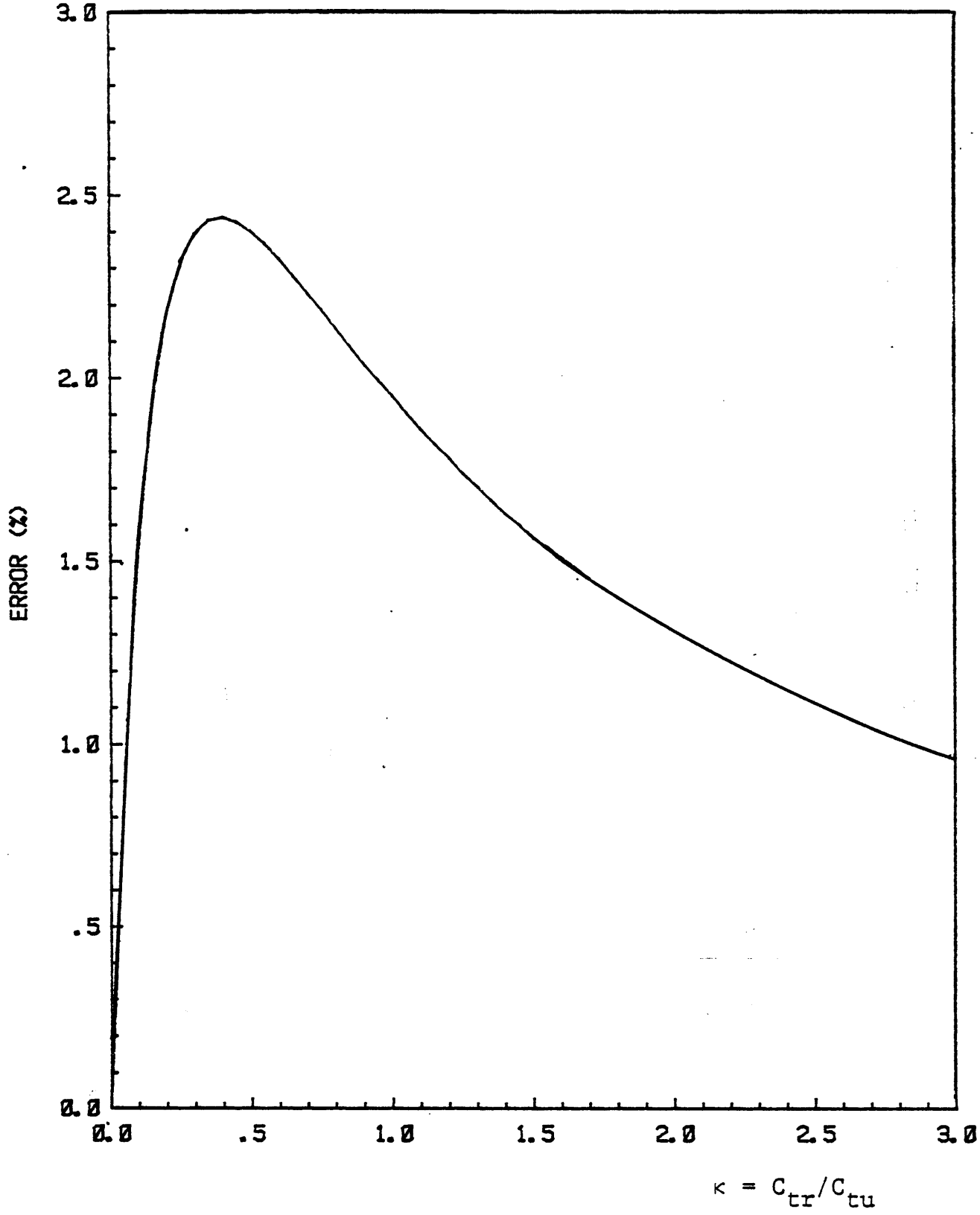

Figure 2-3. Relative error in predicted natural frequency as a function of compliance ratio κ

a simple second-order circuit in terms of preserving the location of the first resonant frequency. Equation (27) implies an equivalent lumped compliance where a fraction $4/\pi^2$ times the total tubing compliance shunts the transducer:

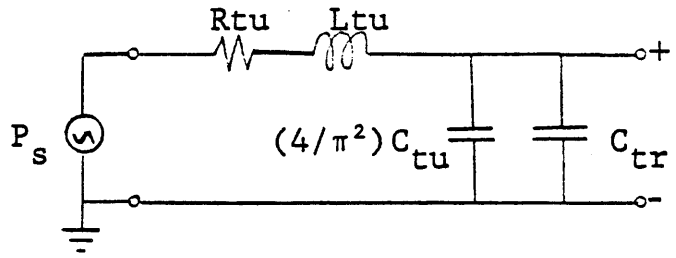

$$C_{eq} = \frac{4}{\pi^2}C_{tu} + C_{tr}$$

with transfer function

$$H(j\omega) = \frac{P_0(j\omega)}{P_i(j\omega)} = \frac{1/(LCeq)}{-\omega^2+(R/L)j\omega+(1/LC_{eq})} \qquad (28)$$

If the resonant frequency of a catheter system is calculated using this lumped model, a useful check on the legitimacy of the assumptions used in constructing the model is to calculate the loss term

$$R'(\omega_r)/L'(\omega_r)$$

to verify the assumption $\omega_r >> R'/L'$ (we still assume $G'=0$). Dividing equation (3b) by (3a):

$$\frac{R'(\omega)}{L'(\omega)} = \frac{\mu}{\rho r^2}\sigma^2 \tan\varepsilon'_0 \qquad (29)$$

so the inequality

$$\omega_r >> \frac{\mu}{\rho r^2}\sigma^2 \tan\varepsilon'_0 \qquad (30)$$

becomes our check on the model assumptions.

2.5 Effect of Trapped Air Bubbles

It has previously been noted that the presence of air in the fluid line remains the single most common cause of low-quality pressure monitoring. This is due to the high compressibility of air relative to water, causing even very small bubbles to greatly increase the total compliance of the system and thereby reduce the resonant frequency. The problem of including air bubbles in our models is exacerbated by the unpredictability of bubble size and location in the clinical setup, and by the strong dependence of bubble compliance on temperature and pressure. The alteration of the normal fluid velocity profile in the vicinity of a bubble may also violate the plane-wave assumption of our model. Nevertheless, we can examine specific situations which are amenable to straightforward analysis and thereby possibly develop some intuition towards the more general situation.

2.5.1 Compliance of Air Bubbles

The compressibility of air depends on temperature, pressure, and molar quantity. The compliance of an air bubble may therefore be expected to vary as pressure waves are propagated in the fluid line. To specify the variation precisely, we need to know the thermodynamic state of the bubble at all times (e.g. isothermal vs. adiabatic compression cycle). We also need to know the temperature variation of air solubility in water and associated time constants to know whether pumping of air into and out of solution with pressure variation is significant. In this study,

we will be content to note the primary effect of static pressure on compliance and ignore all higher-order effects.

If air is assumed to be a ideal gas, then

$$PV = nRT.$$

For a bubble, we will assume n and T are constant. Then

$$PV = K \quad \text{or} \quad \frac{V}{P} = \frac{K}{P^2} \tag{31}$$

If the pressure changes by an infinitesimal amount dP, then the volume changes by an amount dV, with the relation

$$PV = K = (P+dP)(V+dV) = PV + VdP + PdV + dPdV$$

Cancelling like terms and ignoring the higher-order term dPdV, we have

$$dV/dP = -V/P \tag{32}$$

Using the definition of compliance:

$$C = -(dV/dP)$$

and using equations (31) and (32), this becomes

$$C = K/P^2 \tag{33}$$

so we see that the compliance is a strong nonlinear function of pressure. If the pressure excursions inside the fluid column range from 700 mmHg to 1100 mmHg (-60 to +340 mmHg relative to atmospheric pressure), then the bubble compliance may vary between 46% and 118% of its value at atmospheric pressure.

There are several lessons to be learned from this analysis. First, the inclusion of bubbles in the fluid column may cause significant nonlinearities in the frequency response when large pressure excursions are present. Second, at higher static

pressures the effective bubble compliance becomes smaller and therefore the resonant frequency may increase as the static pressure is increased. Henry et al (1967), noting this phenomenon, have even suggested checking the frequency response of the system at high and low static pressures as a means of detecting bubbles in the fluid column. Third, if the pressure excursions are kept small, we may assume a constant compliance for the bubble, considerably simplifying analysis. It is this third approach which we will take in analyzing systems with bubbles in Chapter 4.

Published values of air compressibility at various temperatures and pressures exist. At twenty degrees centigrade and 760 mmHg:

$$dV/dP = 1.0126\times10^{-5}\ Pa^{-1}$$

and

$$C = V\ dV/dP \quad (m^3/Pa) \tag{34}$$

This is the equation we shall use to calculate bubble compliance.

2.5.2 Relationship between Bubble Location and Resonant Frequency

We will now consider how to include a bubble of known volume and location in our lumped element model. The inertance and resistance of the bubble will be taken as negligible, and we will assume therefore that the bubble may be modeled as a lumped compliance shunting the transmission line (we do not make any distinction between bubbles clinging to the wall of the tubing

and bubbles completely occluding the lumen, although there may be reason to do so). We may now view the system as consisting of two transmission lines in series: the first terminating in a lumped compliance (the bubble) and the second in another lumped compliance (the transducer). The analysis of section 2.4 may now be applied, yielding the following model:

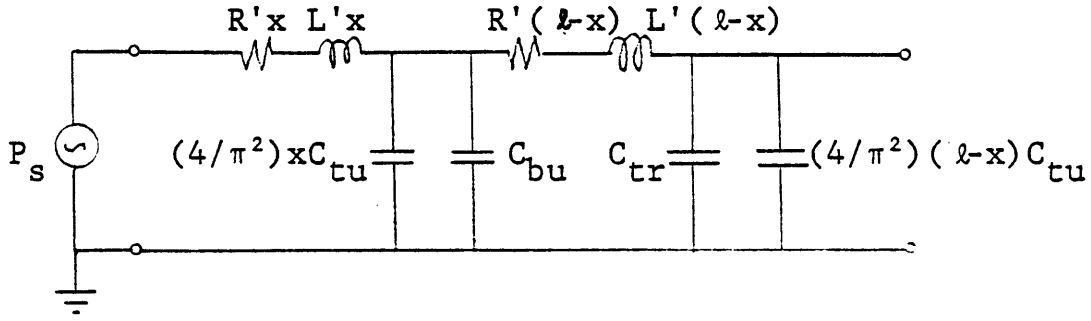

where x=distance from source to bubble and ℓ is the total length of the system. The transfer function governing this circuit is

$$H(j\omega) = \frac{1}{A\omega^4 - jB\omega^3 - C\omega^2 + jD\omega + 1} \qquad (35)$$

a fourth-order equation in ω, where

$$A = x(\ell-x)C_1C_2L^2$$

$$B = 2x(\ell-x)RLC_1C_2$$

$$C = [x(\ell-x)R^2C_1C_2 + L(C_2+xC_1)]$$

$$D = R(xC_1 + C_2)$$

$$C_1 = (4/\pi^2)xC_{tu} + C_{bu}$$

$$C_2 = (4/\pi^2)(\ell-x)C_{tu} + C_{tr}$$

If we assume that C_{bu} is much larger than C_{tu} or C_{tr}, then $C_1 >> C_2$ and the two second-order circuits tend to be decoupled, i.e. they resonate independently. The resonant frequency of the first section is approximately equal to $1/\sqrt{xLC_1}$, so we see that as the bubble is advanced in the tubing towards the transducer (increasing x) the primary resonant frequency decreases. The importance of this result is the recognition that a bubble located in the catheter will not degrade the system performance as much as a bubble located farther up in the system. As a practical aside, we note that when there is suspicion of a bubble causing a low resonant frequency, the search should generally begin at the transducer dome and then proceed backwards toward the catheter.

CHAPTER 3

MATERIALS

All experiments carried out in the course of this study utilized a single brand of pressure extension tubing and two types of pressure transducer. These elements were chosen partly on the basis of availability and partly because they represent typical high-quality components as used by many hospital catheterization laboratories and intensive care units. In addition to these components, a number of additional elements were required in the experimental setup. Hydraulic valves (three and four-way stopcocks) from several manufacturers were used interchangeably. Because of the relative stiffness of the plastics used in these valves, their wide bore, and their small contribution to the overall system length, they were not considered to significantly affect the system response. A pressurized IV bag and standard fluid were used to flush and fill the hydraulic system. Several different pressure sources and flow sources were used as test inputs. A pressure amplifier, CRT display, tape and strip chart recorders, spectrum analyzer, D/A converter, and computer facilities were used to analyze the system dynamics. All of these materials and components are described in more detail below.

3.1 Extension Tubing

The tubing used in this study was obtained from a pressure monitoring kit (HP No. 14233A) marketed by Hewlett-Packard. The tubing is constructed of translucent, high-density polyethylene, with an internal diameter of 1.18 mm, outer diameter of 1.98 mm, and length of four feet (1.22 meter). The ends are supplied with one male and one female luer fitting. No manufacturer technical specifications are available for this tubing, but the characteristic compliance is measured in section 4.1.3. This tubing is relatively stiff compared to similar brands on the market. A previous study by Gardner (1981) of static compliances for commercial pressure tubing lists a range of 1.6 to 17.1 mm^3/100 mm Hg for six feet of tubing, with an average compliance of 7.4 mm^3/100 mm Hg/6 ft. In comparison, the measured compliance of the H-P tubing in these units is 2.72 mm^3/100 mm Hg/6 ft under static conditions and 0.34 mm^3/100 mmHg/6 ft at high frequency.

3.2 Transducers

Two transducers were used in these experiments. The first, a Bentley Trantec Model 800, was generally used as the primary test element in the transducing system because it could be modeled as a pure compliance over a wide range of static pressures. The second, a Hewlett-Packard 1290A, exhibited a fluid leakage phenomenon at lower static pressures which was probably due to movement of fluid trapped between the plastic diaphragm and the quartz transducing element. Since this phenomenon manifests

itself as a frequency-dependent compliance (larger apparent compliance at low frequencies), the 1290A proved undesirable as a primary transducer for these experiments. Instead, the 1290A was used as a reference transducer to monitor the pressure at the input to the extension tubing. In this application, where the transducer effectively shunts the pressure source, compliance is not an important issue. Specifications for the Bentley and H-P transducers list maximum compliances of 0.04 and 0.15 mm^3/100 mmHg, respectively.

3.3 Flush Bag and Fluid

As in a typical hospital setup, the monitoring system was equipped with a means of filling and flushing with fluid. A standard IV bag was filled with a standard fluid (described below) and pressurized to between 200 and 300 mmHg by means of an inflatable bag holder. A length of large-diameter plastic tube and three-way valve connects the flush bag to the rest of the system.

The standard solution consisted of debubbled water, prepared by vigorous boiling. A small quantity of soap solution was added as a wetting agent and all excess air was purged from the bag before pressurizing, thus ensuring a minimum of dissolved air in the fluid. These precautions, coupled with slow, careful filling of the hydraulic system, were found to be of the utmost importance in excluding air from the system. Lack of care in the preparation of fluid or in filling the system invariably resulted in high values of compliance. This solution, developed

after noting that it was virtually impossible to completely eliminate trapped air from the system after filling with saline, was not believed to differ significantly from the physiological saline normally used in terms of its inertial and viscous properties.

3.4 Slow/Fast Flush Unit

A Sorenson Intraflo flush element was included for the experiment involving the system response to a fast flush. The Intraflo and similar units provide a high impedance channel between the flush bag and the catheter, in an attempt to keep the catheter tip free from blood clots. A parallel low-impedance channel can be opened manually to provide a large bolus of fluid for the same purpose (fast flush). The damped oscillations resulting from the release (closure) of this valve were of interest in this study.

3.5 Bench Equipment

Two H-P pressure amplifiers (model 78503C) provided the excitation to and processed the resultant signals from the transducers. The amplifiers were modified for this experiment to provide a flat bandwidth out to 100 Hz, allowing frequency measurements to be made beyond the normal 12 Hz bandwidth of these amplifiers. The reference input excitation to the pressure tubing was provided by a blood pressure simulator (Biotek Model 601). This simulator features a square-wave output for step response measurements, nine selectable pressure waveforms (stored

in read-only memory), manual systolic and diastolic level controls, and provision for an external electrical input. The simulator dome has two ports which connect to the fluid column via luer fittings.

Frequency measurements were made by applying a white noise source to the external input jack of the Biotek simulator. The white noise was amplitude limited to 10 mmHg RMS to approximate small-signal excitation. The pressure transfer function (magnitude and phase measurement) between the reference and test transducers was determined using an H-P Model 3582A Spectrum Analyzer. If desired, the amplifier outputs could be stored on an H-P Model 3960 Instrumentation Recorder and/or a visual record produced on a H-P Model 78172A Chart Recorder. A diagram of the setup is shown in Figure 4-3.

Computational facilities (for modeling purposes) consisted primarily of an H-P Model 85 desktop computer, which has hardwired BASIC as a programming language. The H-P 85 also has an interface bus which allowed it to be used (in conjunction with a digital plotter) to accept spectral and time data from the spectrum analyzer and to produce high-quality graphics on a digital X-Y plotter. For transient analysis, the circuit simulation program SPICE was run on an H-P 3000 series computer.

3.6 Flow Source

For direct measurements of tubing compliance as a function of frequency, a specially designed sinusoidal flow generator was used. The flow source consisted of a commercial microliter

syringe (Hamilton model 7001N) which utilizes a tungsten wire as plunger and is accurate to 0.01 microliter. A custom-made luer adapter allowed the syringe to be tightly coupled to the system under test.

The syringe barrel was rigidly mounted in an aluminum block. The plunger was coupled to a dc servo motor through a mechanical linkage, bearing, and eccentric cam. This arrangement produced a sinusoidal motion of the plunger. The stroke of the syringe could be altered between 0 and 0.8 microliter by varying the eccentricity of the cam with a linear feed screw, and a frequency range of 0.1-14 Hz could be obtained by varying the motor speed. The maximum frequency was conservatively set to limit friction between the plunger needle and barrel, but this range was adequate for our purposes.

3.7 Tap Generator

In order to test the system response to a manually applied impulse, a crude form of a "mousetrap" tapper was designed and built. A schematic representation of the tapper is shown in Figure 3-1. The tapper consists of a platform on which the pressure tubing is secured by two clamps into a milled channel. A tubular steel spring is manually retracted and released. The spring arm passes through its resting position, deforms the tubing (causing a flow impulse as fluid is displaced) and then returns to rest. Because tubing failure from repeated taps was considered a potential problem, the cylindrical spring arm was wrapped with plastic tape to provide a small amount of shock

absorption.

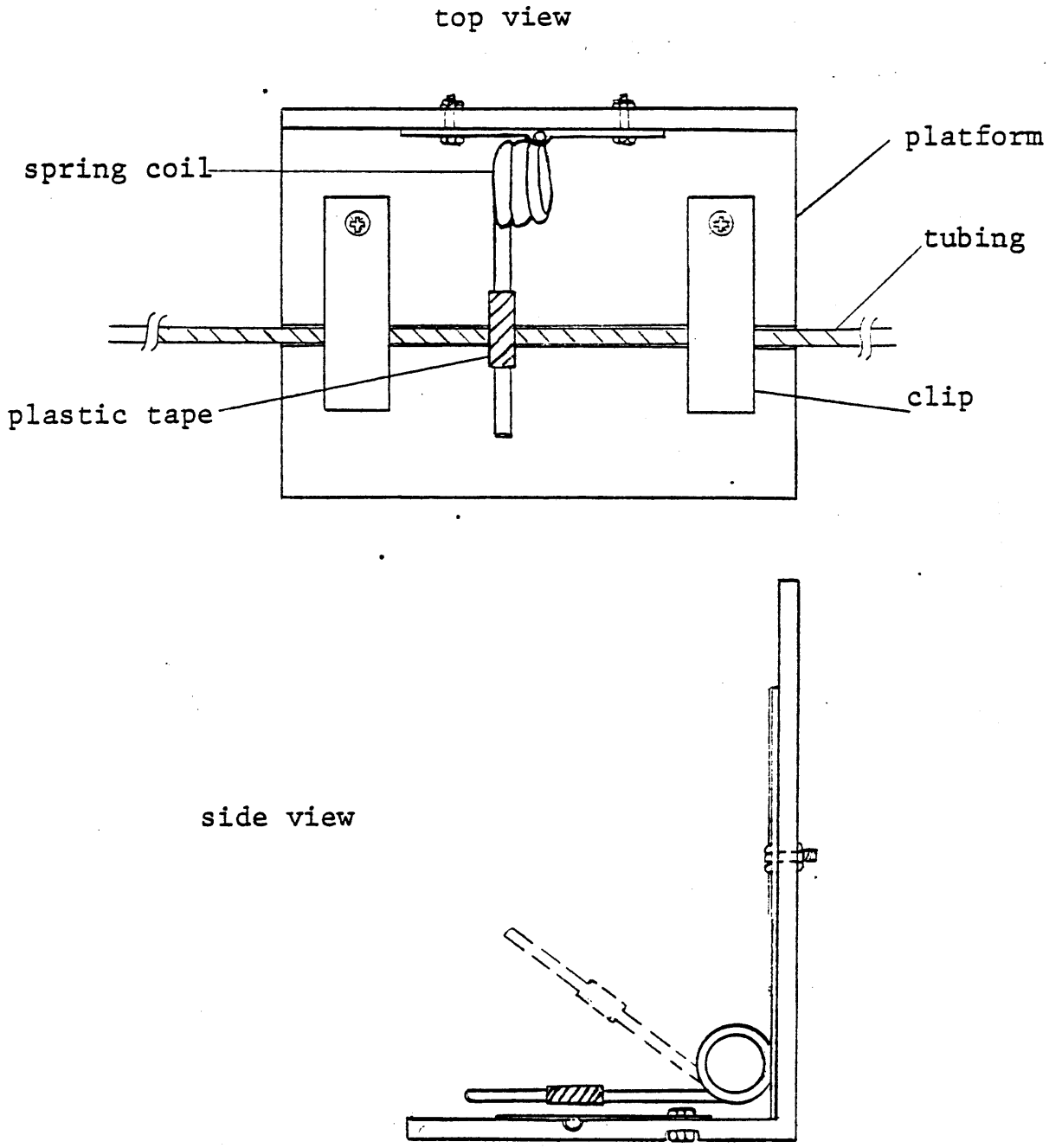

Figure 3-1. "Mousetrap" tap generator

CHAPTER 4

METHODS AND RESULTS

4.1. Determination of Line Parameters

In order to determine the most appropriate model for the transducing system, it is first neccessary to determine the physical parameters which best characterize the separate components of the system. The measured or calculated values of these parameters can then be inserted into the model under examination, allowing comparison between the frequency response of the model and of the experimental system. In some cases (e.g. fluid inertance L) there was no convenient technique available for direct measurement, and some theoretical calculations were of neccessity substituted for direct observation. In other cases (e.g. flow resistance R) the value at zero frequency (steady flow) could be measured but the a.c. value could only be estimated by reference to pulsatile flow theory. The theoretical and experimental values for each parameter are compared whenever possible. Clearly, the use of a flow transducer, which was unavailable, would have been of considerable benefit in this study, since it would have allowed simultaneous a.c. measurements of pressure and flow. Nevertheless, the d.c. measurements obtained represent a positive step towards quantitative analysis and verification of the theoretical models for the pressure monitoring system.

4.1.1 Resistance

Theoretical

Calculating a theoretical value for Rtu actually requires specifying the frequency of interest, since Womersley (1956) has shown the flow resistance to be a function of frequency (see Fig. 2-2). However, at zero frequency Poiseuille's Law applies, and one can write

$$R_{tu} = \frac{8\eta\ell}{\pi r^4}$$

Taking: η =0.001 Pa-sec (approximate for water at 20 degrees C)

ℓ =1.22 meter

r=0.59 mm

We calculate R_{tu} = 2.56×10^{10} Pa-s/m^3.

Experimental

To measure R_{tu}, a calibrated pressure source was attached to one end of the column. The rate of flow through the column was measured by collecting the effluent in a graduated flask and noting the quantity of fluid collected in a given period of time. Invoking the hydraulic equivalent of Ohm's Law, we see that

$$R = P/Q$$

where P represents the source pressure and Q the rate of volume flow. Because there is a source resistance associated with the flush bag and tubing, the resistance measured by this method

represents the sum of the source and load (tubing) resistances. To correct for this, the source resistance (measured by the same technique without the fluid column attached) was subtracted from the total measured resistance. The results of these measurements are shown in Table 4-1. The value for Rtu measured in this way is very close to the theoretical value based on Poiseuille's Law.

4.1.2 Inertance

The calculation of fluid inertance is also dependent on whether a parabolic flow profile (the Poiseuille assumption) is valid or not. The equation for inertance of a cylindrical tube of constant cross-section, derived in section 2.2, is

$$L = \text{fluid mass}/(\text{cross-sectional area})^2$$
$$= \rho\ell/\pi r^2$$

where a multiplying factor of 4/3 must be included at low frequency to account for a parabolic flow profile. Inserting values for fluid volume, density of water, tubing radius and length, we find that

$$L_{tu} = 1.088\times10^9 \text{ Pa-sec}^2/\text{m}^3$$

The value of L_{tu} at resonance will, in general, lie somewhere between this value and the zero-frequency value. Since we are interested in linearizing our model by choosing values for the line parameters that match the true values at resonance, we

measurement	P(mmHg) bag	T(sec)	Q(mm^3)	Q(mm^3/sec)	R(mmHg-sec/mm^3)
flush bag only	77	10	7850	785	.0981
bag and tubing	150	10	5500	550	.2727
	95	10	3250	325	.2923
	90	10	3570	357	.2521
				average	.2724 +/- .0201

$$R_{tu} = R(\text{bag+tubing}) - R(\text{bag only})$$

$$= .1743 \text{ +/- } .0201 \text{ mmHg-sec/mm}^3$$

$$= (2.32 \text{ +/- } 0.26) * 10^{10} \text{ Pa-sec/m}^3$$

equivalent circuit:

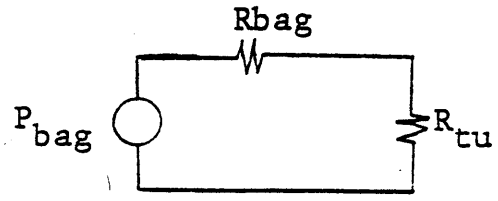

Table 4-1. Tubing resistance measurements

need to know the location of the natural frequency of our model before we can specify a value for L using equation (3a). However, since this value will determine a new natural frequency in equation (27), we need to resort to an iterative technique to determine a value for L_{tu} that satisfies both equations (3a) and (27). So long as convergence of the iterative procedure occurs (unproven in theory), there are no anticipated difficulties.

4.1.3 Compliance

Theoretical

Determining a theoretical value for the compliance of plastic pressure tubing is quite difficult, since the tubing exhibits viscoelasticity (wall loss) and creep (plastic flow) which makes the compliance complex and frequency dependent. The classical formula for compliance of a thick-walled tube, equation (5) may be cautiously applied and expected to be reasonably valid at higher frequencies, where creep (but not wall loss) may be neglected. Substituting in these approximate values:

$E = 1.72 \times 10^8$ Pa
$r = 0.59$ mm
$h = 0.40$ mm
$l = 1.19$ m
$s = 0.46$

we can estimate C_{tu} as

$$C_{tu} = 3.25 \times 10^{-14} \text{ m}^3/\text{Pa}$$

Experimental

To directly measure C_{tu} (as well as C_{tr}) as a function of frequency, the flow generator described in section 3.6 was used. The system was assembled as depicted in Figure 4-1, taking extreme care to exclude air from the system and tighten all couplings, since even microbubbles in the filling solution will cause large errors in compliance measurement. The transducer compliance was directly measured by calculating the ratio of applied volume increment to observed change in pressure (see Table 4-2). The compliance was relatively independent of frequency over the frequency range tested, with an average value of 2.68×10^{-15} m^3/Pa, well within the manufacturer specifications for this transducer. This result gave some degree of confidence that extraneous sources of compliance had been eliminated.

The total compliance of the parallel combination of transducer and extension tubing was then measured between 0.12 and 13.2 Hz, and Ctu calculated as

$$C_{tu} = C_{total} - C_{tr}$$

where C_{tu} is taken to be independent of frequency. A strong frequency dependence was noted (see Figure 4-2) with the tubing becoming increasingly stiff as the frequency was increased. By curve-fitting and extrapolation, C_{tu} for very low and very high frequencies could be estimated. A high frequency compliance of 1.95×10^{-14} m^3/Pa (the curve has apparently reached a limiting

value by 13.2 Hz) was used for all subsequent models, since this represents the value in the frequency range around resonance, and for the purposes of this study we can tolerate inaccuracies in component values at low frequency.

One assumption which should be justified at this point is that the frequency range over which these measurements were made is well below the resonant frequency of the system. This assumption is critical because the effect of tubing impedance and reflections near resonance results in a change in the effective compliance (i.e. the tubing can no longer be treated as a lumped element). Fortuitously, the compliance of this tubing reached a limiting value well below the assumed natural frequency of the system (f_n>50 Hz), so treating the tubing as a lumped compliance in this measurement appears to be justified.

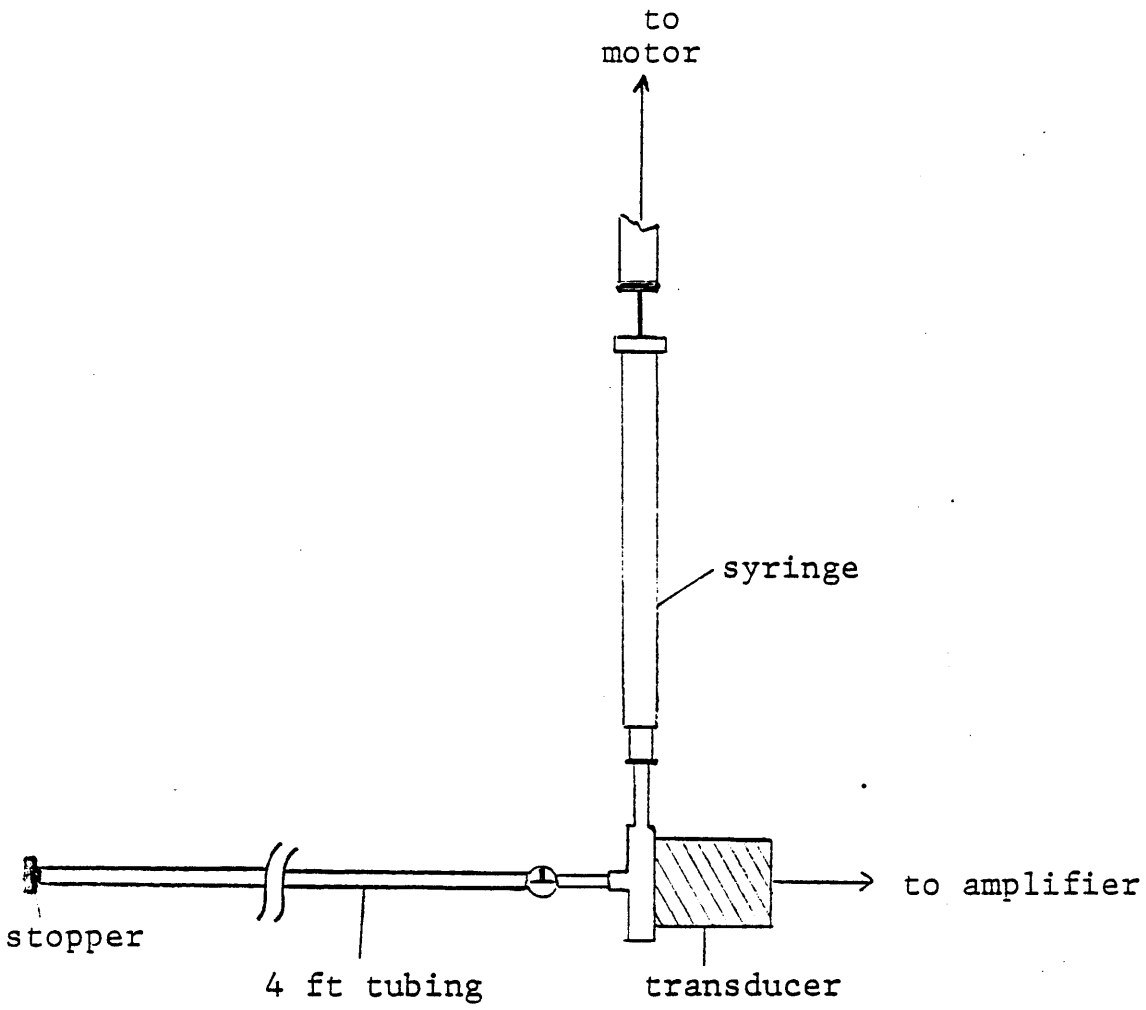

Figure 4-1. Setup for direct compliance measurement

Test	Stroke (ΔV)	Frequency (Hz)	P (mmHg)	C (mm^3/100mmHg)
transducer only	0.04 mm^3	0.20	112	0.0357
		1.25	115	0.0348
		1.60	115	0.0348
		2.75	115	0.0348
		4.50	117	0.0342
transducer + tubing	0.20 mm^3	0.12	11.6	1.724
		0.92	16.4	1.219
		1.20	18.4	1.087
		1.83	22.0	0.909
		3.00	30.0	0.667
		4.05	37.4	0.535
		5.25	44.0	0.455
		13.20	70.0	0.290

Table 4-2. Tubing compliance measurements

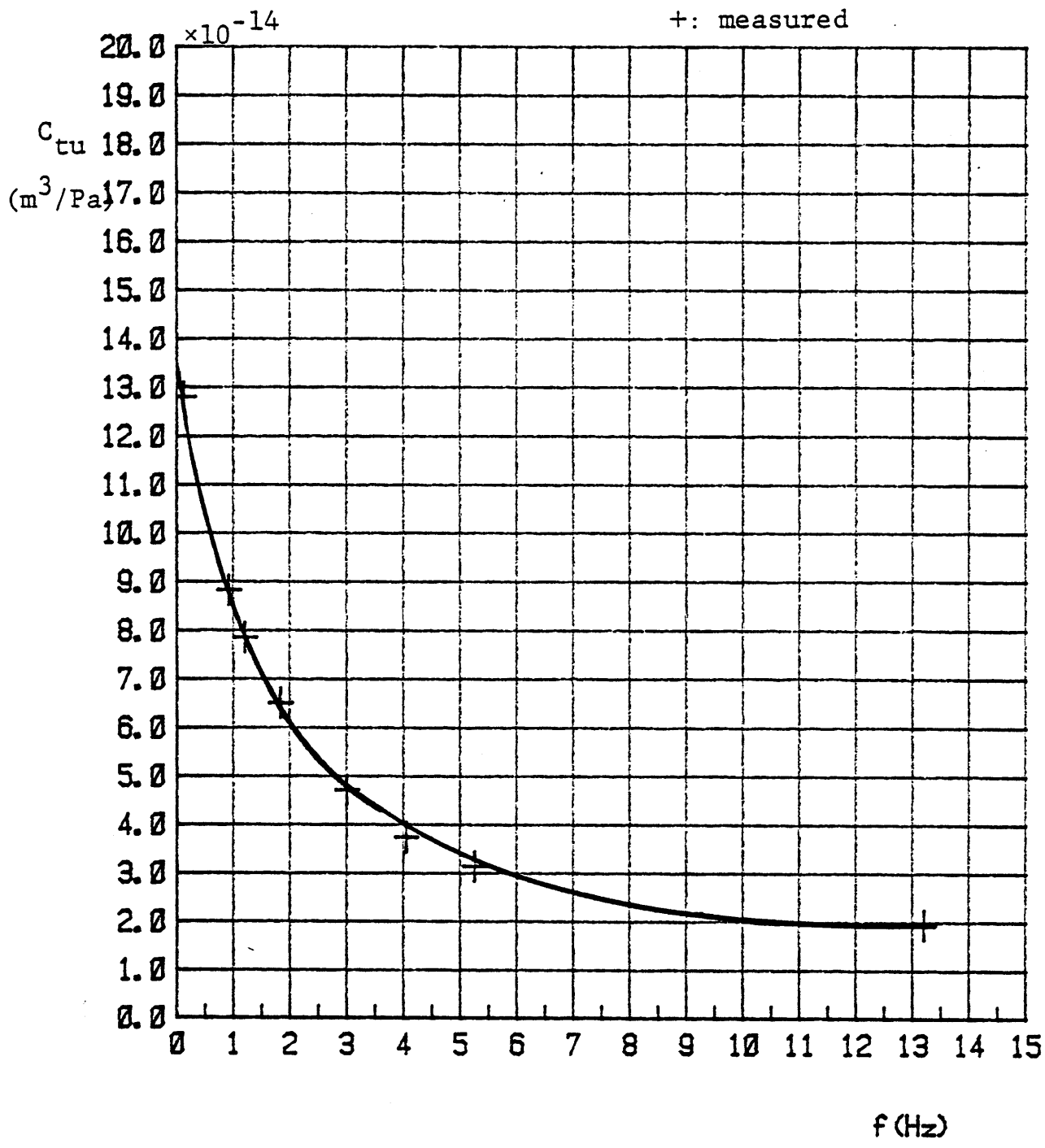

Figure 4-2. Tubing compliance vs frequency

4.2 Determination of Resonant Frequency for the Bubble-free System

4.2.1 Experimental

To test the validity of the lumped-parameter model in terms of predicting the resonant frequency of the monitoring system, the experimental frequency response was compared with theory using the measured or inferred values of the line parameters. The system shown in Figure 4-3 was assembled, and the frequency response measured using the white noise source and spectrum analyzer at a static pressure of 50 mmHg. The system was verified as being bubble-free by remeasuring the frequency response at a static pressure of 150 mmHg and noting no apparent change in the frequency response. Because the compliance of an air bubble is strongly dependent on the applied pressure, the effect of increasing the static pressure on a system with bubbles will be a decrease in the effective compliance and thus a shift in resonance to a higher frequency, as has been shown by Henry et al (1967). The gain and phase of the transfer function at both values of static pressure is shown in Figure 4-4. We note that an artifact is present at about 56 Hz. This artifact, which is seen in all spectra presented in this work, is the result of carrier noise generated within the pressure amplifiers. This noise is unavoidable since the amplifiers are being used far beyond their design bandwidth, but fortunately did not occur at a frequency which was of major importance in our study.

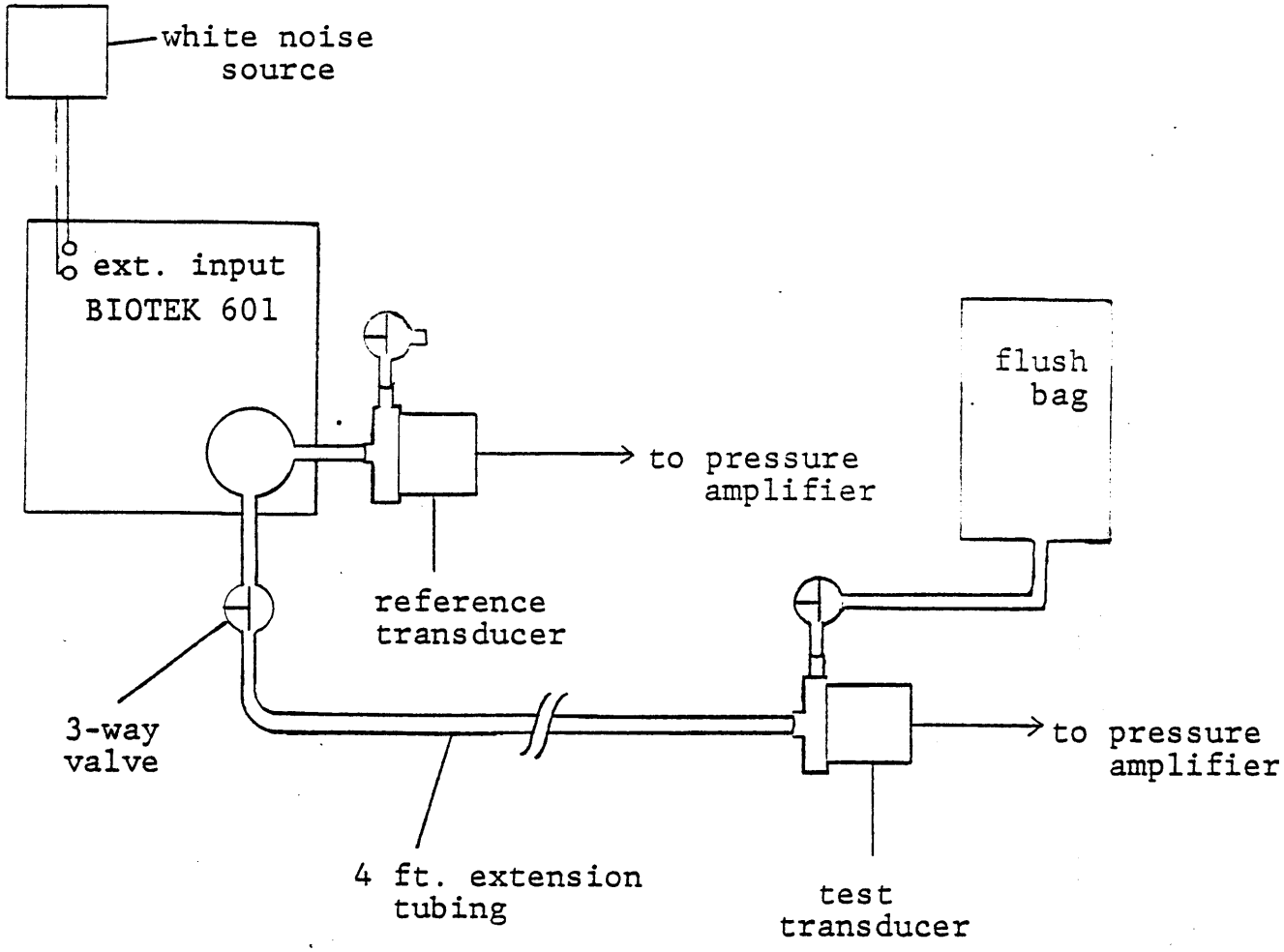

Figure 4-3. Diagram of laboratory setup for testing of catheter system

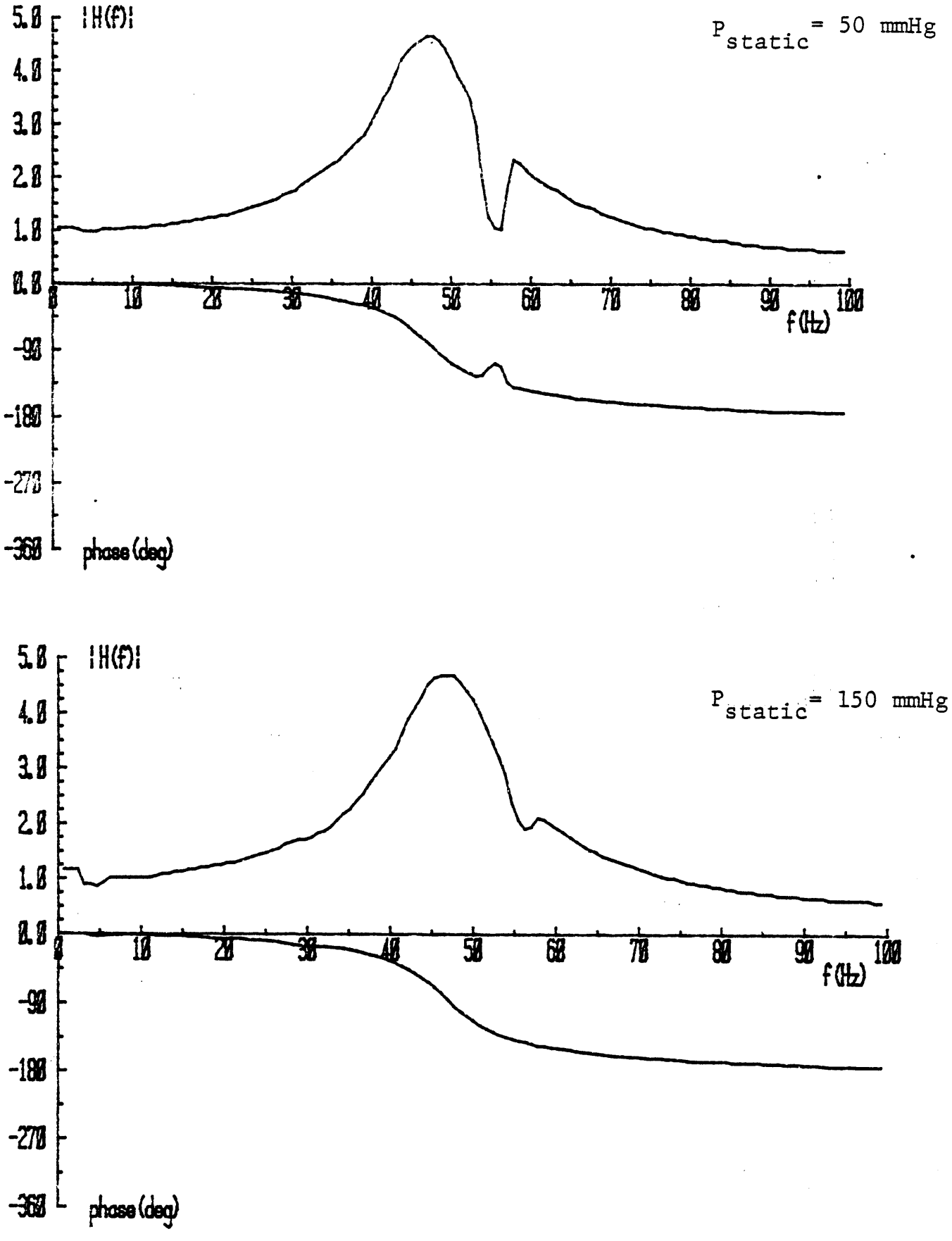

Figure 4-4. Transfer function for the bubble-free system

4.2.2 Theoretical

To locate the resonant frequency of the second-order model, we need to simultaneously solve equations (3) and (27) for Rtu and Ltu (Ctu and Ctr are assumed constant at 19.5 and 2.68×10^{-15} m^3/Pa , respectively). Starting with an initial guess at the resonant frequency of the model allows calculation of R and L, and the two sets of equations can then be solved iteratively until R and L (and ω_n) converge. Convergence has not been shown to be guaranteed, but we experienced no difficulties in computing a convergent solution. The values for R, L, f_n, and D (damping coefficient) found by this method are:

$f_n = 45.78$ Hz

$R_{tu} = 5.561 \times10^{10}$ Pa-sec/m^3

$L_{tu} = 1.265 \times10^{9}$ Pa-sec^2/m^3

$D = 0.0761$

The frequency response of the second-order system with this natural frequency and damping coefficient is shown in Figure 4-5 with the experimental curve superimposed. The agreement is fairly good considering the many approximations involved in constructing the model and the possible errors in measuring the compliance of the tubing (extraneous sources of compliance tend to make our measurements high). Our check on the assumption of low loss, equation (30), becomes

$$\omega_r >> \frac{\mu}{\rho r^2}\sigma^2 \tan\varepsilon_0$$

287.6 rad/sec >> 43.9 rad/sec

which is not a bad approximation.

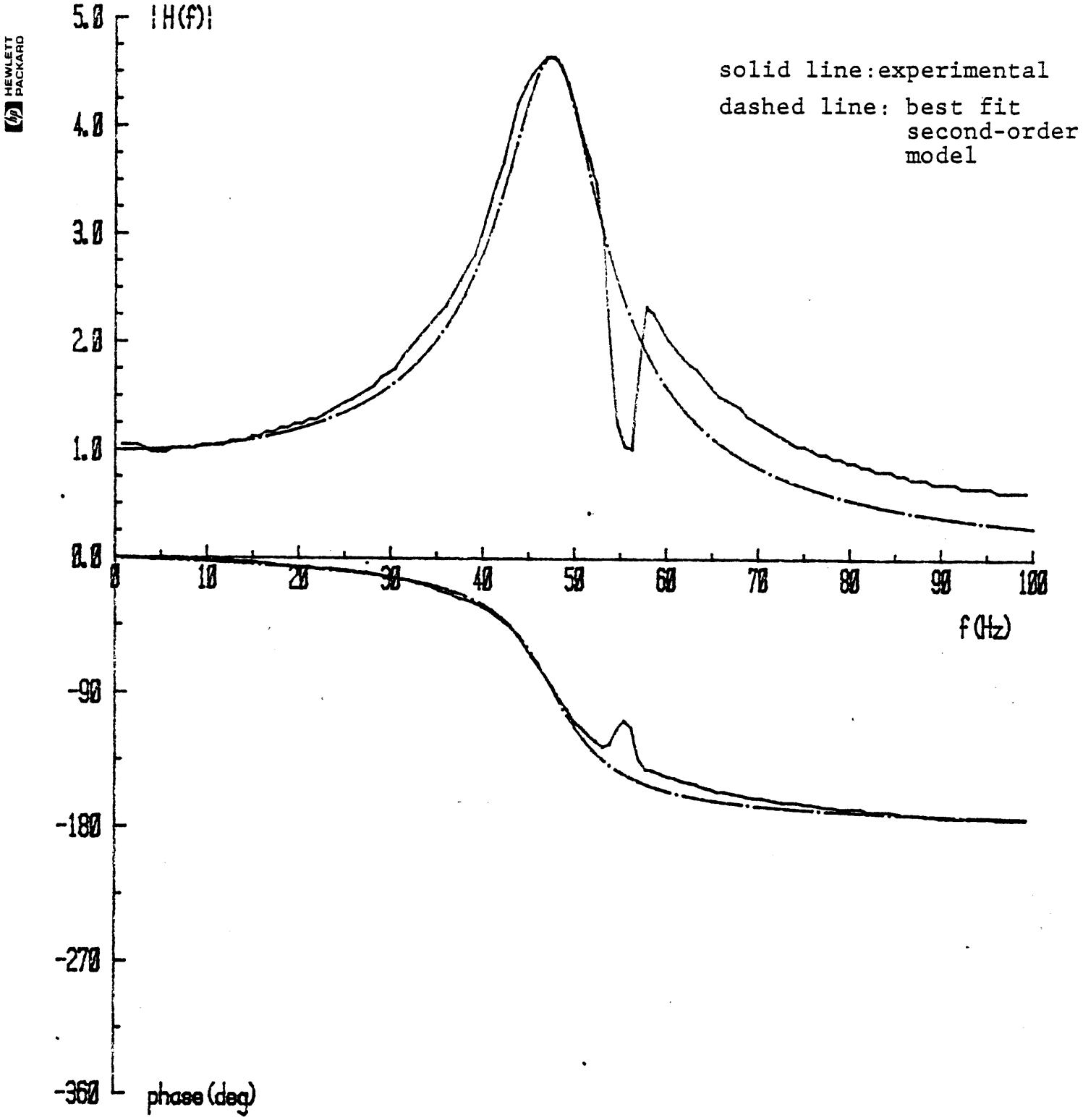

Figure 4-5. Comparison of second-order model with experimental transfer function

4.3 Air Bubble Experiments

4.3.1 Resonant Frequency as a Function of Bubble Location

The development of section 2.5 has suggested that the presence of a bubble in the pressure tubing may be represented by a parallel lumped compliance introduced at the appropriate point in the transmission line model of the system. A desirable simplification was then to theoretically separate the transmission line into two sections, pre- and post-bubble, and model each section as a second-order circuit. This leads to a cascade of two R,L,C circuits whose transfer function is a fourth-order equation in ω (see equation (28)). The frequency response of this fourth-order system exhibits two resonant peaks, a dominant (primary) peak at a lower frequency and a secondary peak at a higher frequency. Since from a practical point of view it is the primary resonance which is of interest, the main result of this theory is that, for a bubble of given size, the primary resonant frequency decreases as the bubble is advanced in the tubing towards the load (transducer) end.

To test this theory, we measured the frequency response of our standard system as a bubble of known volume was advanced in the tubing by means of controlled flushing. The response function of the system was measured using the 3582A Spectrum Analyzer and noise source as in the previous experiment. First, the system was carefully filled with the standard solution. The frequency response was then measured at static pressures of 50 and 150 mmHg and compared to verify the absence of any bubbles. Next, a bubble

of known volume at atmospheric pressure (29.0 mm^3) was introduced at the Biotek dome and advanced through the fluid column by slow flushing. The frequency response of the system was measured with the bubble located at various points (20, 40, 60, 80, and 122 cm) along the fluid column. The response functions are shown in Figure 4-6(a)-(f). To compare these results with the theory of section 2.5.2, the theoretical response functions are also plotted in Figure 4-6. Note that the higher-than-predicted damping at higher frequencies tends to obscure the second resonant peak in the magnitude plot, but the phase plot clearly shows the 180 degree phase shift around the natural frequency.

For the tubing line constants, Rtu and Ltu were allowed to vary with the excitation frequency according to equation (3) and the bubble compliance was calculated using equation (34). Note that the model tends to overestimate the high frequency resonance and underestimate the damping. There is no obvious explanation for the former result. The latter is most likely due to nonnegligible wall loss (viscoelasticity) in the tubing, which our model ignores. The qualitative agreement, however, is encouraging, for it supports the view of the bubble as "decoupling" the fluid line into two sections, each of which may be approximated by a lumped second-order circuit.

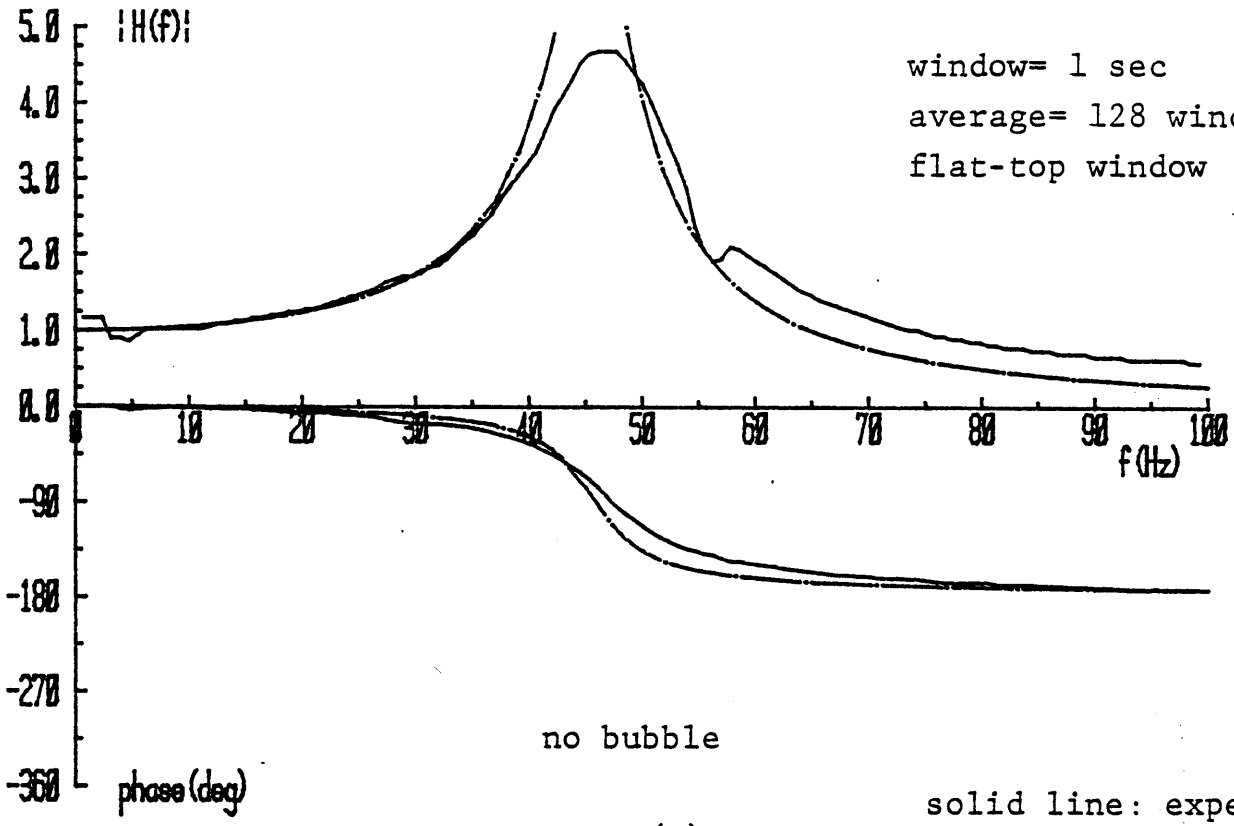

(a)

solid line: experiment
dashed line: theoretic

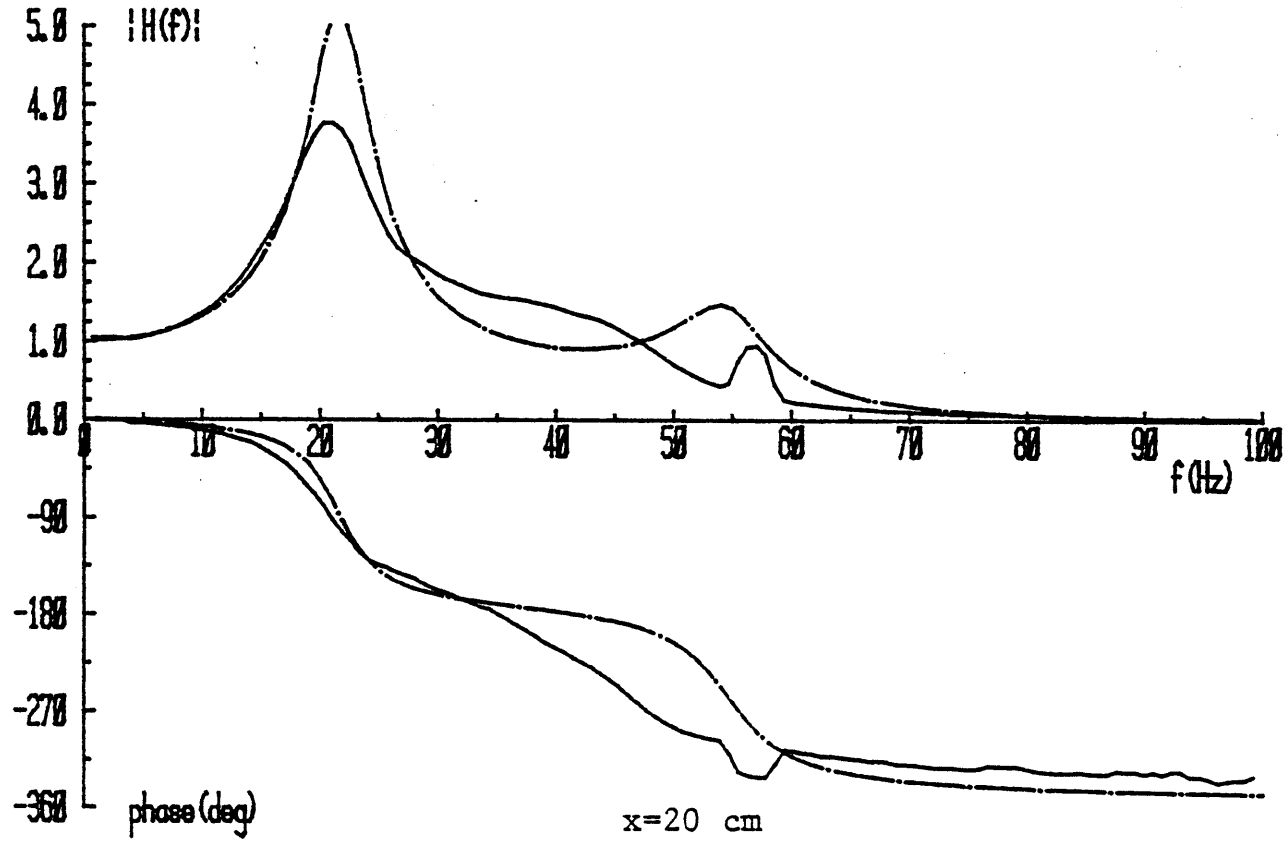

(b)

Figure 4-6. Model and experimental transfer functions

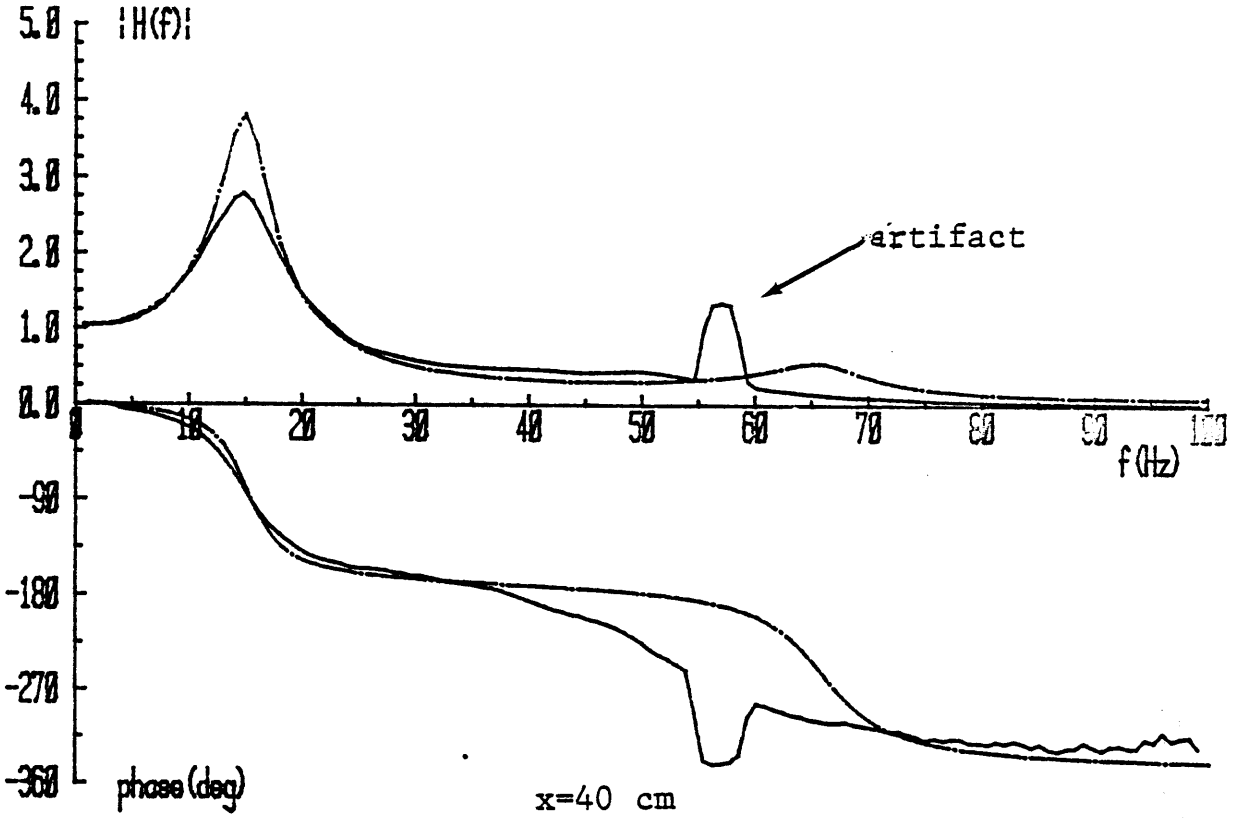
|H(f)|
5.0
4.0
3.0
2.0
1.0
0.0
-90
-180
-270
-360
artifact
f(Hz)
phase(deg)
x=40 cm

(c)

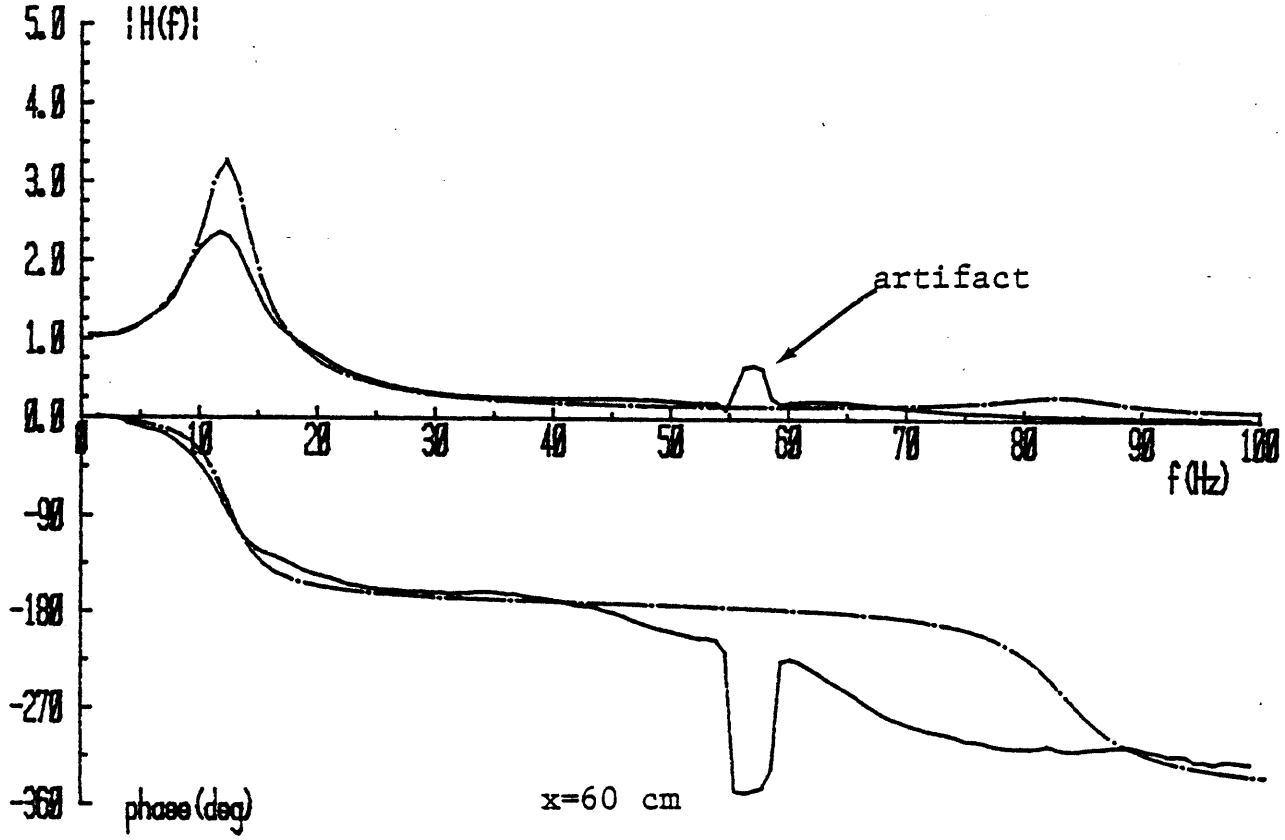
|H(f)|
5.0
4.0
3.0
2.0
1.0
0.0
-90
-180
-270
-360
artifact
f(Hz)
phase(deg)
x=60 cm

(d)

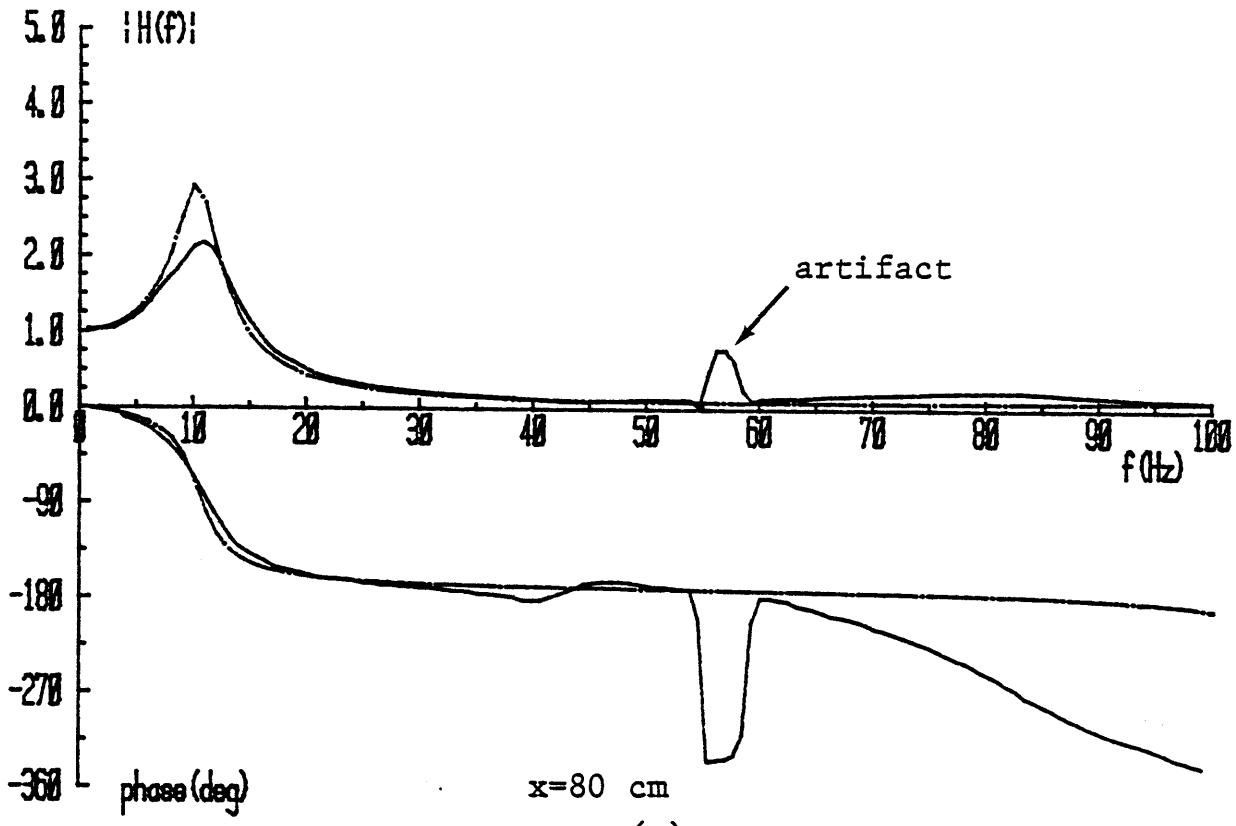
5.0
4.0
3.0
2.0
1.0
0.0
-90
-180
-270
-360
|H(f)|
artifact
10
20
30
40
50
60
70
80
90
100
f(Hz)
phase(deg)
x=80 cm

(e)

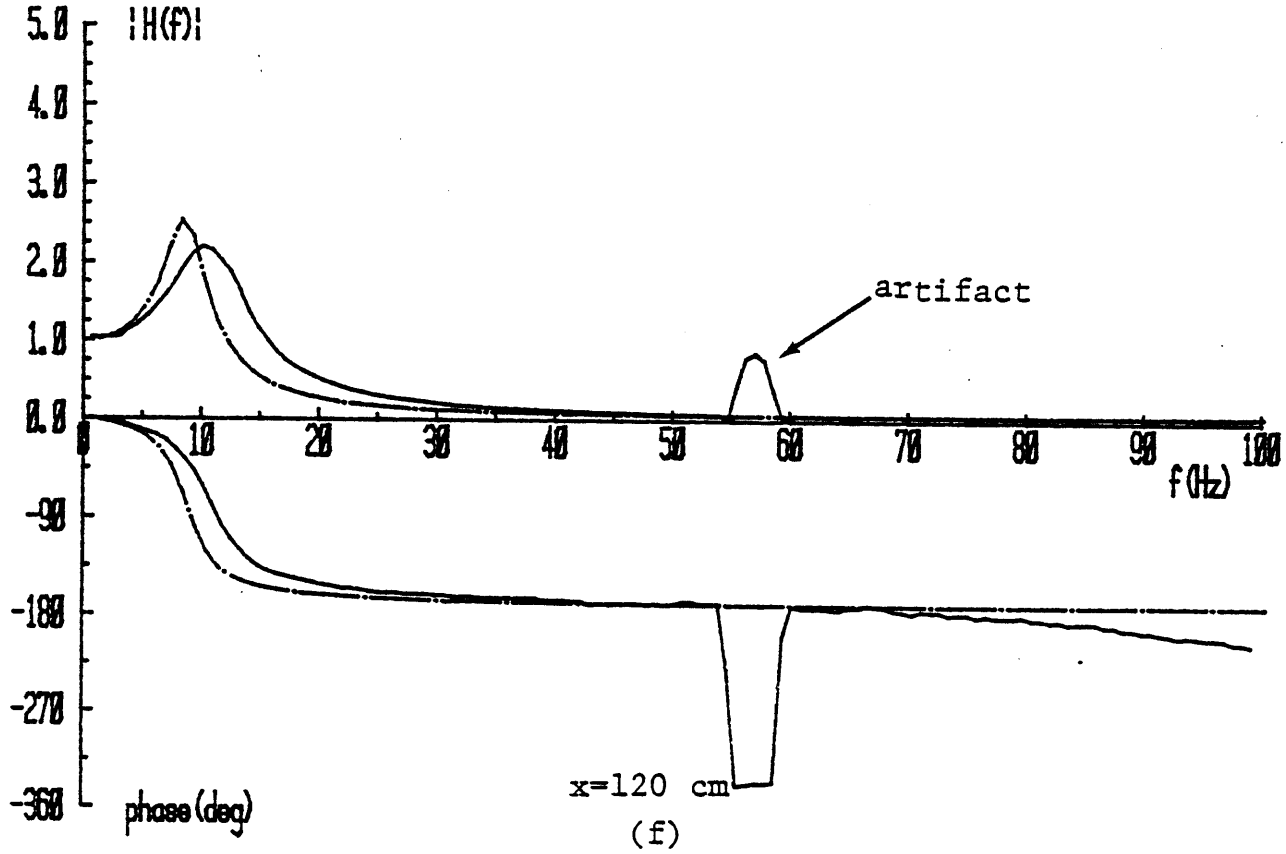
5.0
4.0
3.0
2.0
1.0
0.0
-90
-180
-270
-360
|H(f)|
artifact
10
20
30
40
50
60
70
80
90
100
f(Hz)
phase(deg)
x=120 cm

(f)

4.4 Tap and Flush Experiment

The theoretical development of Chapter 2 has suggested that most catheter systems may be approximated by a limited number of lumped sections, the number of sections neccessary depending on bubble distribution within the system but perhaps practically limited to two or three. This lumped model has had the feature of simplifying system analysis at the expense of absolute accuracy. In terms of deducing the system response function $H(\omega)$ from the time response to a known input (typically a pressure step at the patient end of the catheter), many researchers have shown the lumped second-order model to be adequate. This is because, in most cases, even a rough knowledge of the location of the first resonant frequency and damping coefficient may be sufficient to judge the adequacy of the system or even to attempt frequency compensation via impedance matching. Often, discovery of a lower-than-expected resonant frequency may result in a search for occult air bubbles rather than inverse filtering of the pressure waveform or other electrical technique which requires fairly precise knowledge of the transfer function.

The clinical unsuitability of the "pop" technique and other inputs which require access to the catheter tip led us to examine two alternate methods of exciting the natural frequencies of the system which do not require withdrawal of the catheter. The first method, tapping the extension tubing with a small mechanical device, represents an attempt to provide an impulse of pressure to the system. The other, approximating a pressure step, is the

"flush" technique recommended by Gardner (1970,1981). This technique is quite convenient in that the flush device is normally present as part of the monitoring setup. We tested both of these excitations on debubbled systems as well as those containing a bubble to determine two things:

(1) Is the time or frequency response independent of the location of the input?

(2) Is the primary resonance of the system, as seen from the normal pressure source (the catheter tip), sufficiently excited by the input to be detected?

4.4.1 Experiment

The experimental system set up to answer these questions is depicted in Figure 4-7. Two sections of the H-P pressure tubing were connected in series with a three-way valve, allowing a bubble to be introduced into the side port of the three-way valve. This was done because the side port is a typical site of bubble entrapment and also to prevent the bubble from being swept out of the tubing during the "fast-flush". A Sorenson Intraflo flush unit was connected between the transducer and tubing (the normal clinical location), and the Biotek pressure simulator connected to the other end of the tubing.

The system was filled with the standard solution in the usual manner, and the transfer function measured at P_{static} = 50 mmHg and again at 150 mmHg to verify the absence of trapped air (see Figure 4-8(a)). The response of the system to the following

four excitations was then tested:

(1) Biotek square wave (the model excitation)

(2) Tap at x=20 cm

(3) Tap at x=224 cm (l-x=20 cm)

(4) Flush

Typical response waveforms are shown in Figure 4-9(a)-(d).

The lack of accurate calibration of the force delivered by the tap device, possible motion artifact of the tubing during the tap and flush procedures, and other problems serve to make rigorous analysis of these responses exceedingly difficult. Nonetheless, the following qualitative analysis may be useful:

(1) The Biotek step response was consistently the most artifact free. Determination of resonant frequency and damping from the peaks of the time response was relatively easy and matched the spectrum analysis determined previously;

(2) The fast-flush response was relatively artifact-free, although care had to be taken to avoid disturbing the tubing during the maneuver. The initial "spike" artifact in the response could not be used for analysis;

(3) The tap response invariably produced some high-frequency oscillation which made determination of f_n and D much more difficult. It is not known whether this is due to motion artifact of the tubing, phase cancellation resulting from a secondary wavefront (the impulse can propagate in both directions away from the tap), or perhaps even another mode of wave propagation in the

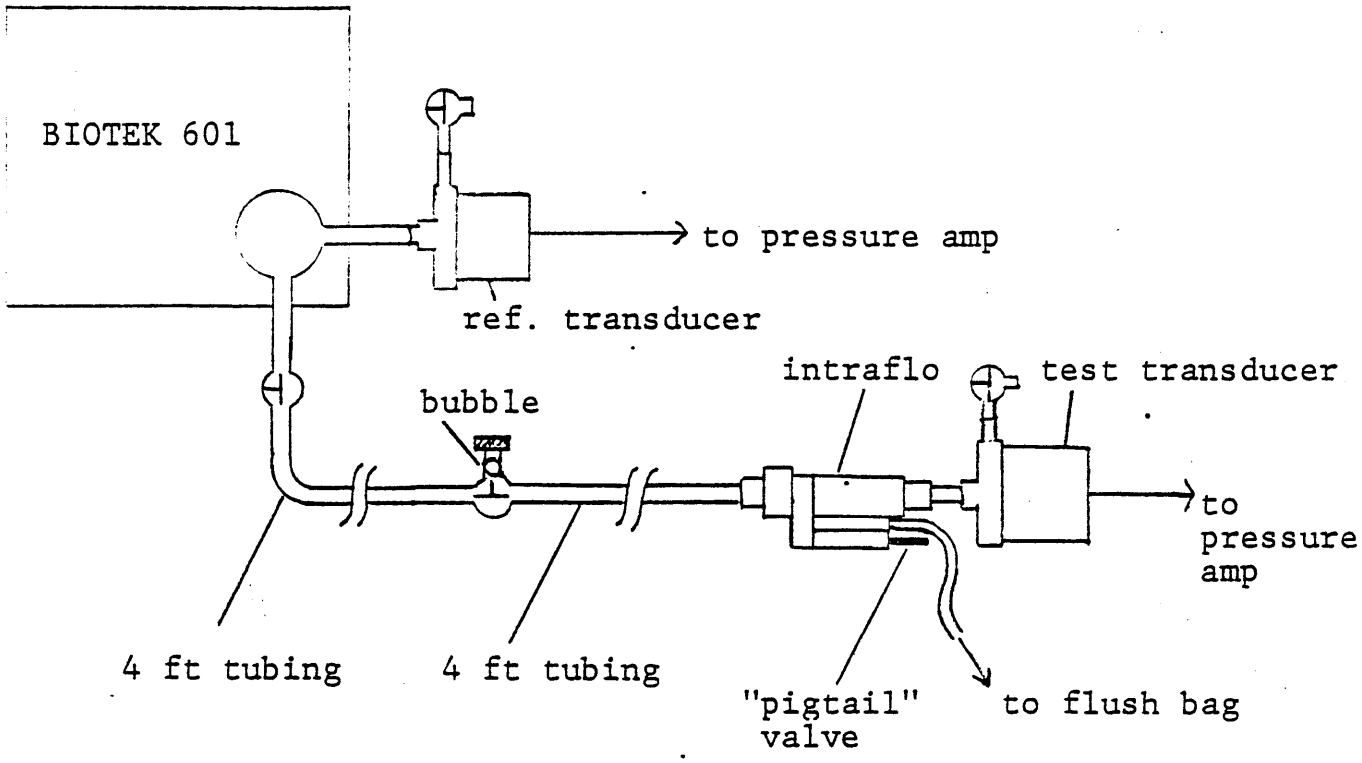

Figure 4-7. Diagram of setup for tap and flush experiments

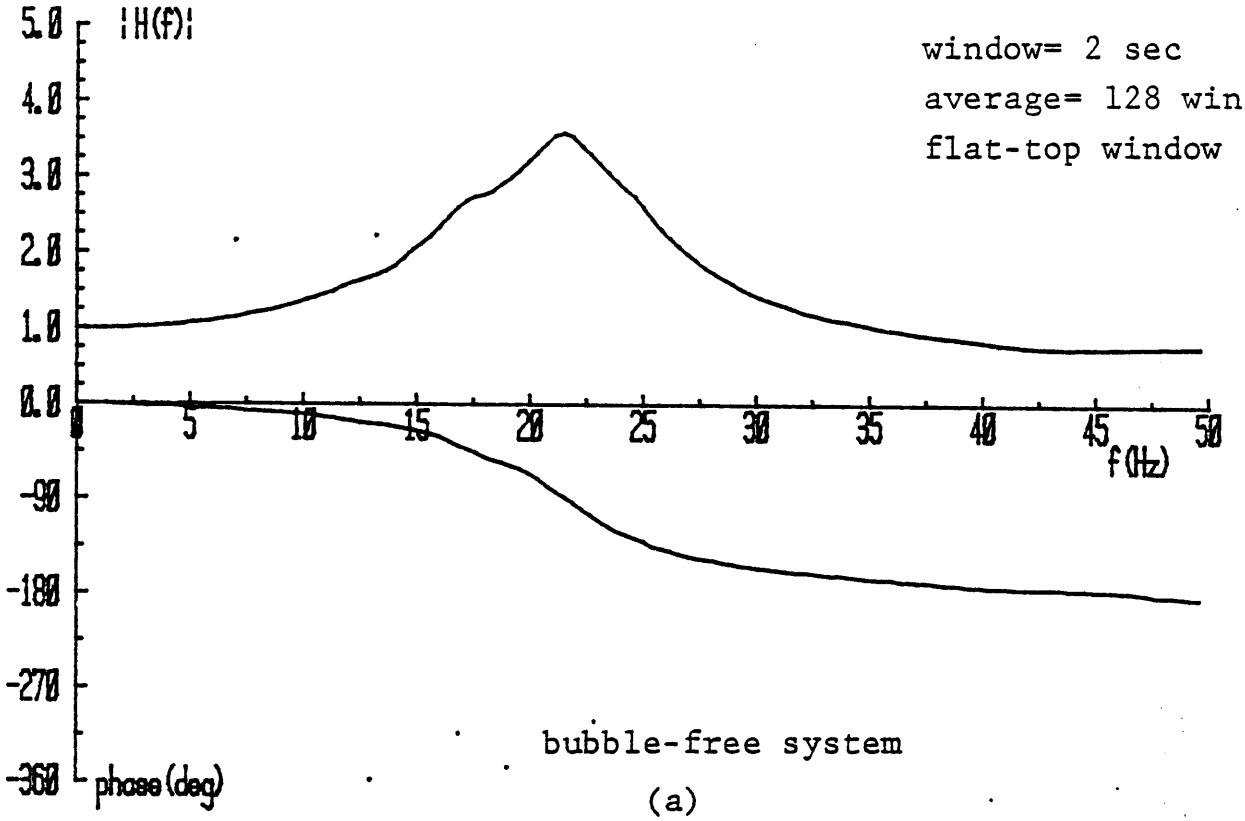

bubble-free system

(a)

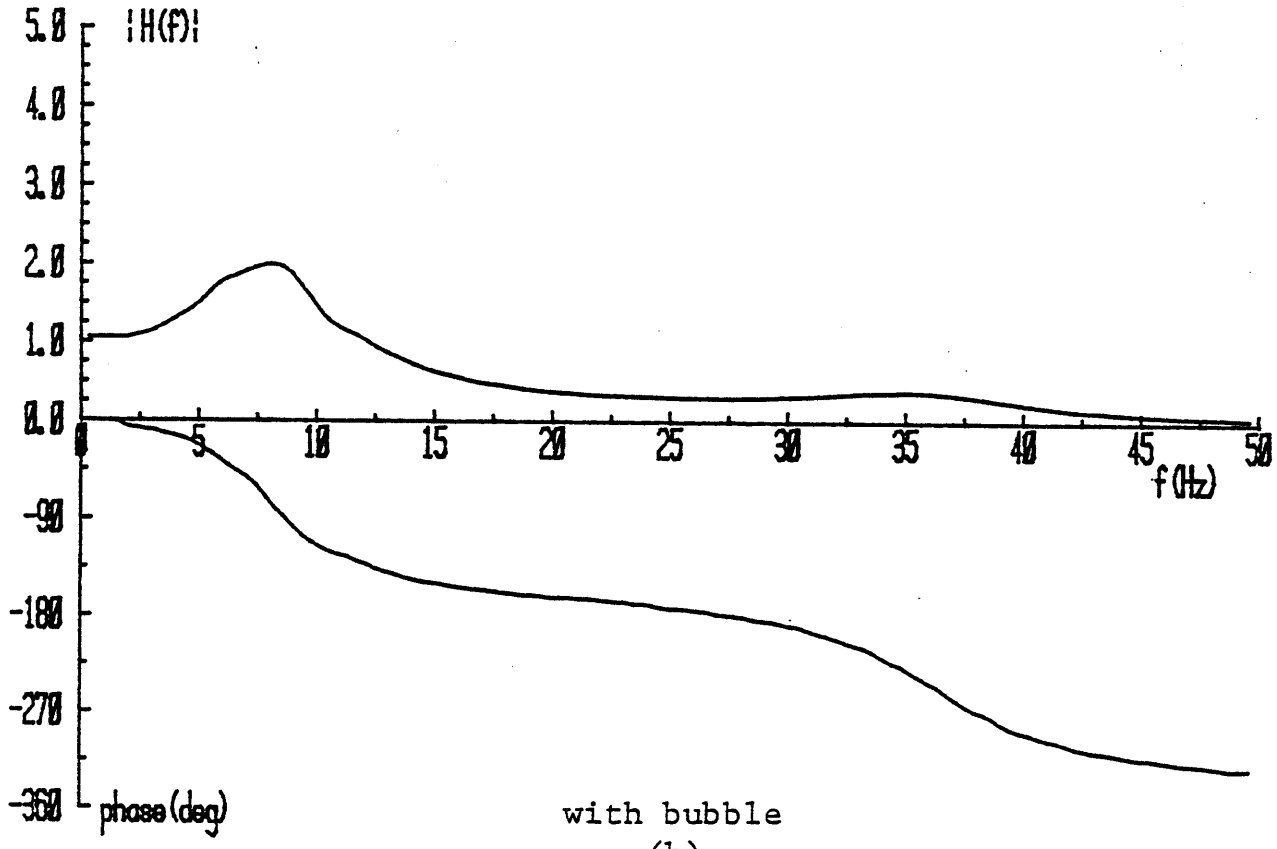

with bubble

(b)

Figure 4.8 Transfer function with and without bubble

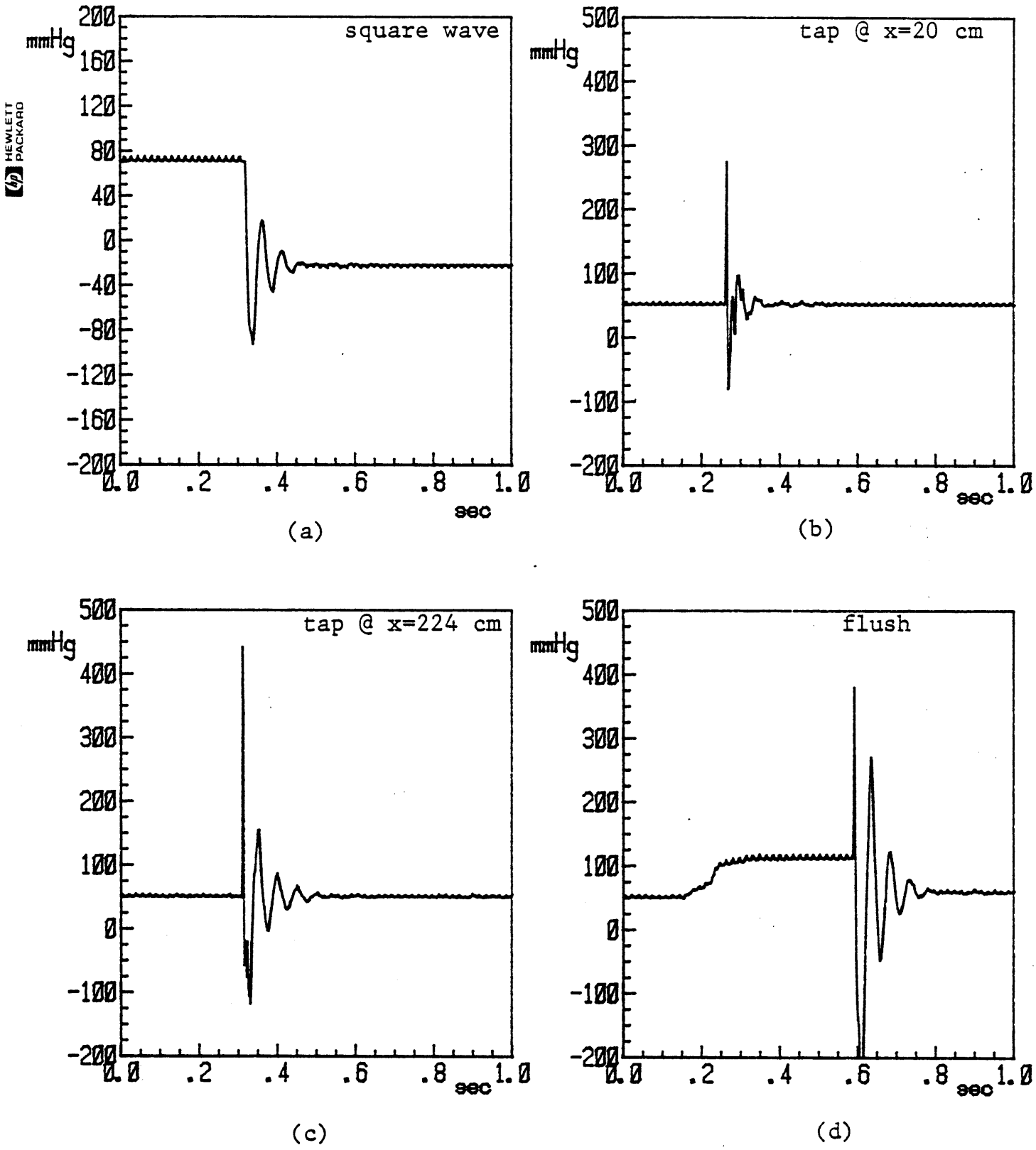

Figure 4-9. Square-wave, tap, and flush responses for bubble-free system

tube wall itself. We also observed that the tap response became greater in amplitude as the tap site was moved closer to the transducer, possibly because of the attenuation produced by wall loss in the line.

A considerable change in the responses to these excitations occurred when a bubble was inserted into the side port of the three-way stopcock connecting the two lengths of tubing. The transfer function of the system with bubble (Figure 4-8(b)) exhibits the predicted decrease in resonant frequency and appearance of a second frequency peak. The Biotek continued to produce a response from which the lower resonant frequency and damping were easy to deduce (Figure 4-10(a)). The tap responses (Figure 4-10(b)-(c)) unfortunately are dominated by oscillation at the higher resonance, leading to the tentative conclusion that the tap is an inadequate excitation for the primary resonance.

The flush response has components at both the secondary and primary frequency, as is seen in Figure 4-10(d). However, further experimentation revealed that the high frequency response is not due to the flush itself. Rather, it is due to the manner in which the flush valve in the Intraflo closes. The release of the "pigtail" which opens the valve actually produces a flow impulse in the tubing as the rubber membrane which valves the flow reseats. This can be shown by repeating the flush experiment with equal pressures in the flush bag and tubing. Upon release of the flush valve, the piston-like action of the rubber membrane produces the high-frequency response shown in Figure 4-10(e).

Comparing Figures 4-10(d) and (e), it appears that most, if not all, of the high-frequency oscillation produced by the fast-flush is due to the mechanics of valve closure in the Sorenson unit and not from the initial conditions set up by steady-state flow. Unfortunately, other makes of flush device were not tested to determine if they were more suitable for this purpose.

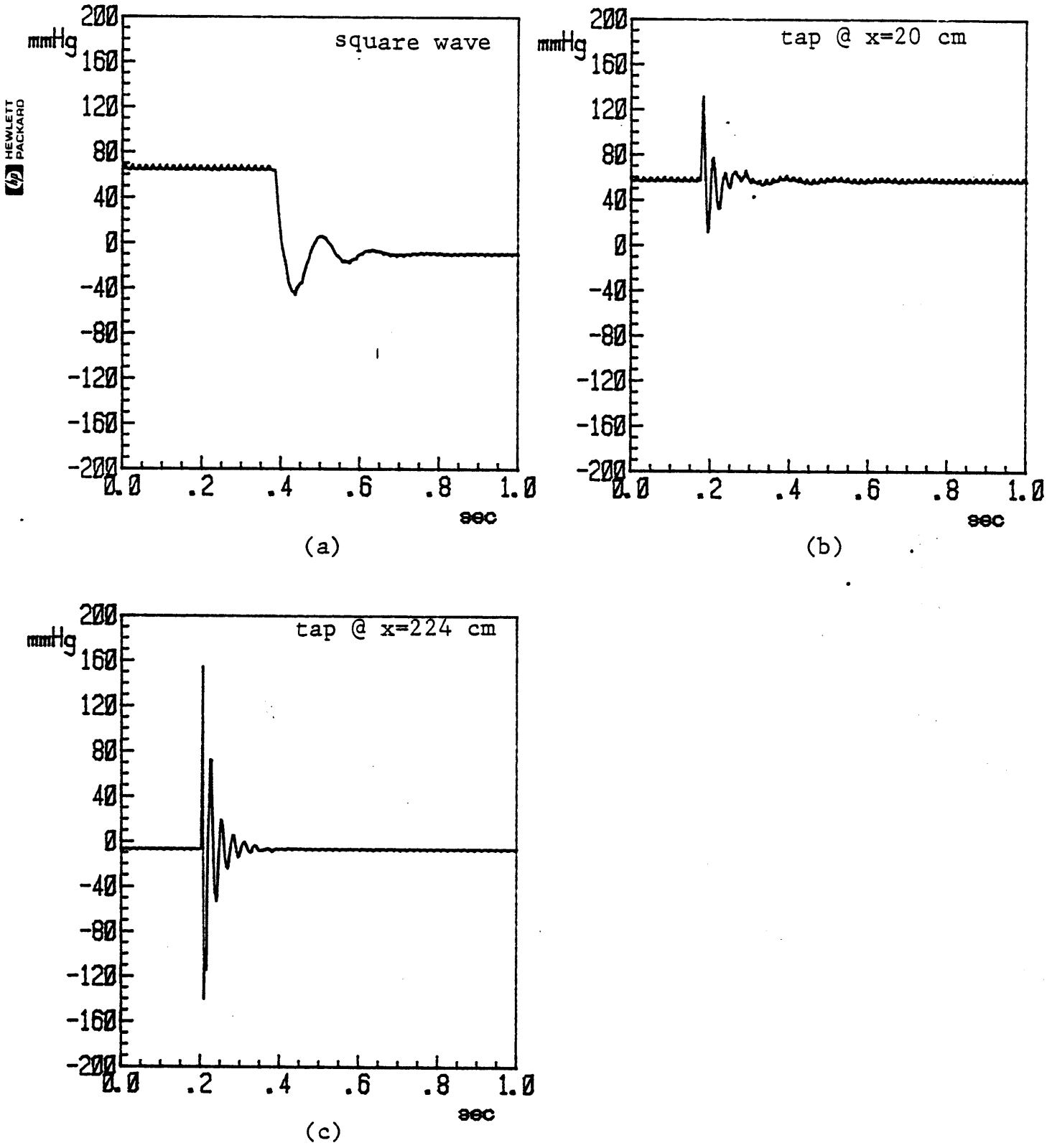

Figure 4-10. Square-wave, tap, and flush responses with

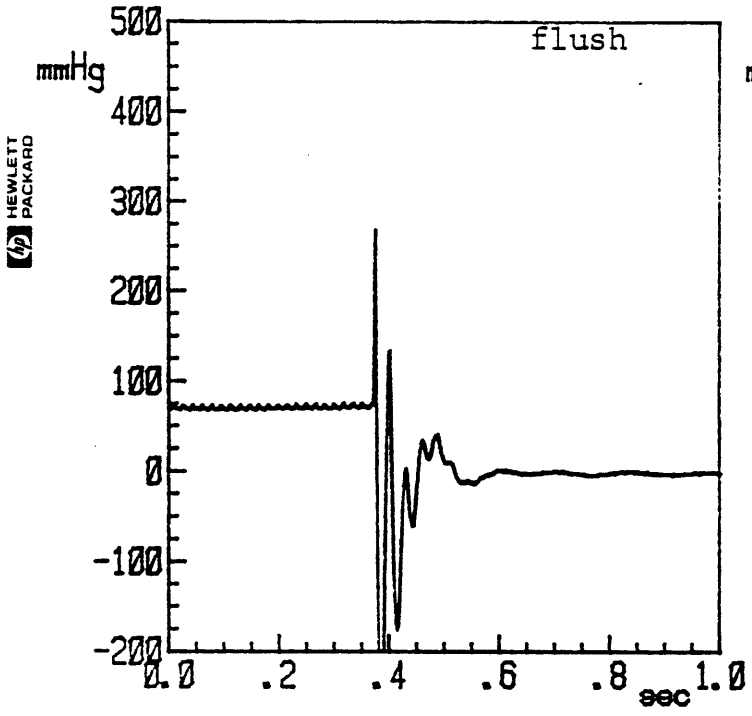
flush
mmHg
500
400
300
200
100
0
-100
-200
0.0
.2
.4
.6
.8
1.0
sec
HEWLETT PACKARD

(d)

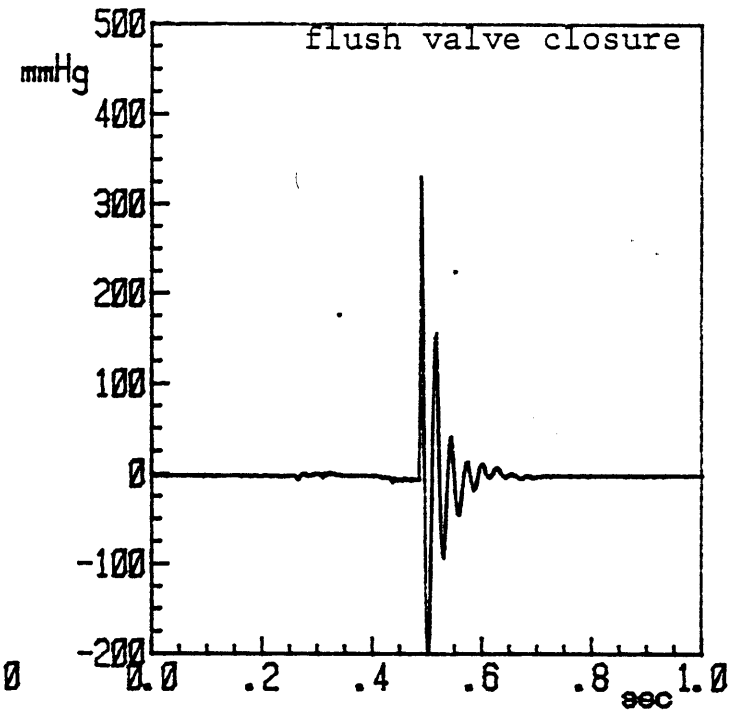
flush valve closure
mmHg
500
400
300
200
100
0
-100
-200
0.0
.2
.4
.6
.8
1.0
sec

(e)

CHAPTER 5

DISCUSSION

We have gone to considerable lengths in this study to develop a lumped-element model for the catheter system that is a good approximation to the more accurate transmission line approach through the first resonant frequency, and then to experimentally demonstrate its validity. It may be argued that this analysis was not really neccessary to achieve our purported objective of finding an *in vivo* method of measuring frequency response. We feel, however, that the effort put into modeling has at least paid off in developing a rationale for understanding the relative importance of tubing, transducer, and bubble compliances in determining the primary resonant frequency of a system of given dimensions. The analysis has also served to suggest the range of component (R, L, and C) values for which the lumped approximation is a good one.

Having justified the use of a lumped second-order model to represent the catheter system tested in this study, we then proceeded to demonstrate how an occult bubble causes decoupling of the fluid column into pre- and post-bubble sections, with the result that the column may have significant resonances at more than one frequency. This result is crucial to our understanding of the role that location and energy distribution play in the response to tap and flush inputs. We can now examine these results in more detail.

5.1 Tap and Flush Responses

The results of section 4.4 strongly suggest that the tap excitation leads to response artifacts. This is not entirely surprising for two reasons: first, the impulse has to be transmitted through the tubing wall, which may cause longitudinal wave propagation in the wall, temporary narrowing of the lumen due to relaxation effects, and other wall related phenomena; second, the impulse is a signal which requires very large forces to transfer significant energy to the system - the large pressure variations in the tubing make transmission nonlinearities more likely to be evident in the response. Even though we discovered an alternate flow impulse source - the flush valve - which may eliminate some of the problems of the "mousetrap" method (tubing effects) it still seems impossible to circumvent the nonlinearity problems.

Another problem with the tap excitation is location sensitivity. As we have seen, pre- and post-bubble excitations give qualitatively different responses. This may possibly be the result of reflection from the impedance mismatch existing at the bubble and high-frequency attenuation in the tubing. The impedance mismatch will tend to limit the amount of energy transferred through the bubble and thus isolate the two halves of the system. The attenuation makes it difficult to achieve an appreciable response without using extremely high forces. Moreover, the energy is very localized within the tubing, intuitively making the lumped-element model seem unsuitable. All of these considerations combine to make the tap an unattractive

method of excitation.

On the other hand, we have found evidence to suggest that the flush excitation (although perhaps not the particular flush device tested) may give results similar enough to the "pop" technique to justify its use in the clinical setting. We can justify the similarity of the flush and pop responses using the lumped model and energy considerations. First, consider the circuit shown below, which represents a d.c. model of our previous catheter system containing a bubble mid-tubing (component values typical of our experimental system):

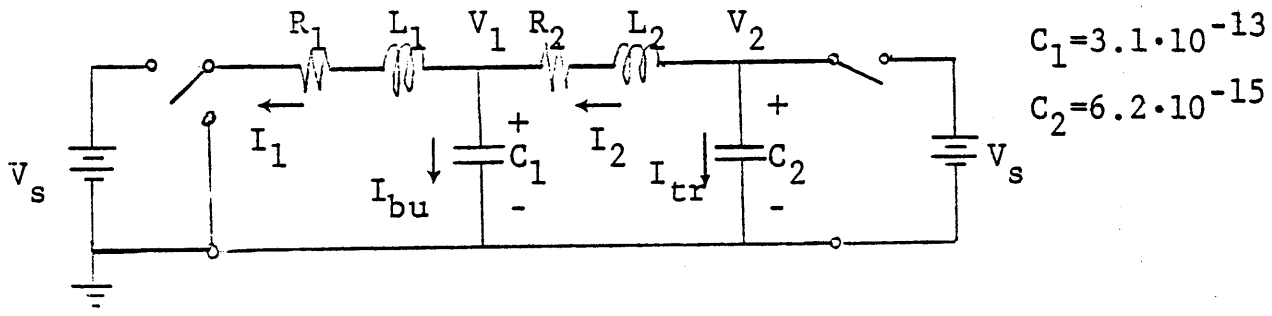

where we have substituted V and I for P and Q respectively to avoid confusion between electrical charge and hydraulic flow.

We can consider the pop and flush excitations as setting up certain initial conditions in the line and then allowing the system to decay. This corresponds to the homogeneous (unforced) solution to the coupled differential equations governing the fourth order circuit:

$$(L_1C_1s^2 + R_1C_1s - 1)V_1 + (L_1C_2s^2 + R_1C_2s)V_2 = 0$$

$$-V_1 + (L_2C_2s^2 + R_2C_2s + 1)V_2 = 0$$

5.1.1 Initial conditions

The initial conditions set up by the pop excitation are:

$$I_1 = I_2 = I_{bu} = I_{tr} = 0$$

$$V_1 = V_2 = V_s$$

which means that all the energy is stored in the compliances. For the flush, we have

$$I_1 = I_2 = \frac{V_s}{R_1 + R_2} = I_s; \quad I_{bu} = I_{tr} = 0$$

$$\tilde{V}_1^2 = 2\int_0^{.5} V_s^2 x^2 dx = V_s^2/12$$

$$\tilde{V}_2^2 = 2\int_0^{.5} V_s^2 x^2 dx = 7V_s^2/12$$

where we have represented the pressure as a linear function of the distance x along the fluid column and computed the average square of the pressure within each section. The reason for this will be evident shortly.

Now, we can determine the approximate distribution of energy within the system under each set of initial conditions. The total energy stored in each section is

$$E = \frac{1}{2} \Sigma C_i V_i^2 + \frac{1}{2} \Sigma L_i I_i^2 \qquad i = 1,2.$$

For the pop excitation, there is no flow, and the pressure is independent of location. Since $C_1 >> C_2$ (commonly the case even

with small bubbles), the majority of the energy in the system is stored in the bubble. Therefore the response is primarily the decay of the left-hand RLC circuit. Since the lowest resonance tends to be associated with the bubble, this means that the response will in most cases be approximately second order.

For the flush, there is kinetic energy in the fluid motion and potential energy in the compliances. Using the component values shown,

$$E_{kin_1} = E_{kin_2} = 0.5L_1I_s^2 = 0.5\frac{V_s^2L_1}{R^2} \cong 4.8\times10^{-13}V_s^2$$

$$E_{pot_1} = 0.5C_1\tilde{V}_1^2 = (1/24)C_1V_s^2 = 1.3\times10^{-14}V_s^2$$

$$E_{pot_2} = 0.5C_2\tilde{V}_2^2 = (7/24)C_2V_s^2 = 1.8\times10^{-15}V_s^2$$

We see that for the component values chosen (typical for the system we have studied) the majority of the energy is stored in the fluid motion and not in the compliances. Therefore the initial energy stored within each section is approximately equal.

5.1.2 Transient solution

Given these initial conditions, we can determine the transient solution to the ideal pop and flush inputs. However, this will require recomputing the line parameters R and L, since these are frequency dependent. These were estimated from the observed location and height of the resonant peaks in the

experimental data (Figure 4.7(b)) as:

$R_1 = 1.5 \times 10^{10}$ Pa-sec/m^3

$R_2 = 2.8 \times 10^{10}$ Pa-sec/m^3

$L_1 = 7.0 \times 10^{8}$ Pa-sec^2/m^3

$L_2 = 6.3 \times 10^{8}$ Pa-sec^2/m^3

A transient solution with these parameter values and the initial conditions determined from the d.c. equivalent circuit was determined using the SPICE circuit simulation program. The transient solution from 0 to 400 milliseconds for the pop test initial conditions is shown in Figure 5-1 and for the flush test in Figure 5-2. As expected, the pop test causes almost an entirely low-frequency resonating response, while the flush test yields a response that is a mixture of the low- and high-frequency resonances. The low-frequency response, however, is easy to distinguish, particularly since the high-frequency oscillations are quickly damped. This is to be expected, both because the damping increases with frequency and because the damping is defined as loss/cycle, not loss/time. The higher damping and faster oscillation of the high-frequency resonance guarantees that it will decay faster than the low-frequency oscillations, so we may reasonably expect the low-frequency response to dominate. This lends some support to our assertion that the flush excitation is a satisfactory input for determining the low-frequency resonance. Rothe and Kim (1980) have observed

that the flush waveform produced by the snap of the Sorenson Intraflo valve excited primarily the extension-tube-to-transducer part of their catheter system, not the entire system including catheter. While we have not tested entire systems containing long catheters, it seems likely, in view of our test results and analysis, that it is the flow impulse caused by the snap of the Intraflo valve that produces the high-frequency oscillations noted in this study and in the work of Rothe and Kim. The flush method itself appears to be otherwise sound.

How may these results be extended to more general situations (different component values, more bubbles in the tubing)? We have outlined a general method for attacking this problem although we have only computed a solution for one particular system. It should not prove too difficult to model any specified system in terms of lumped sections in a similar manner. An interesting extension of this work would be to determine a "worst-case" response - one that contains resonances close enough together to make the decoupling assumption poor.

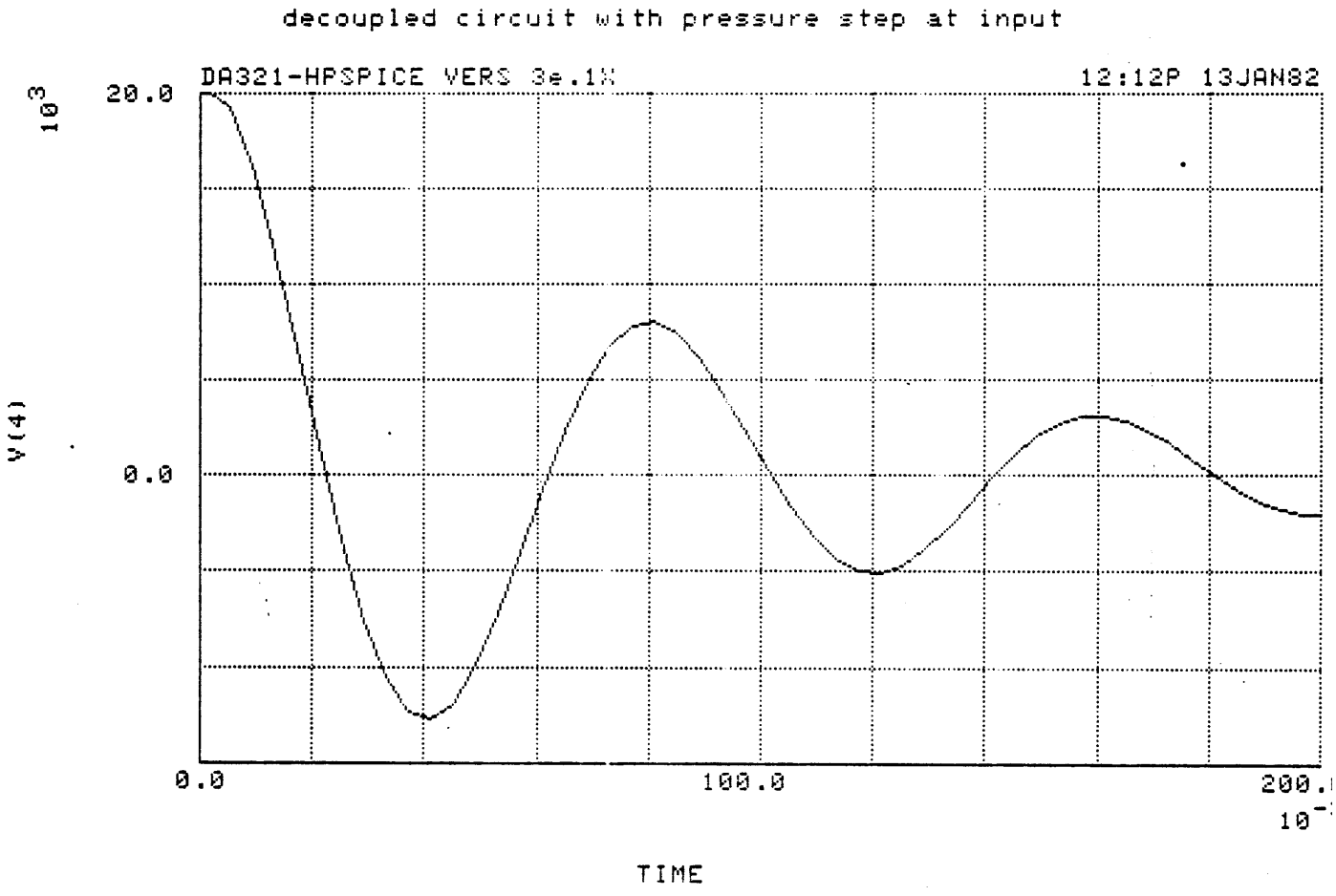

Figure 5-1. Simulated response to pressure step at input

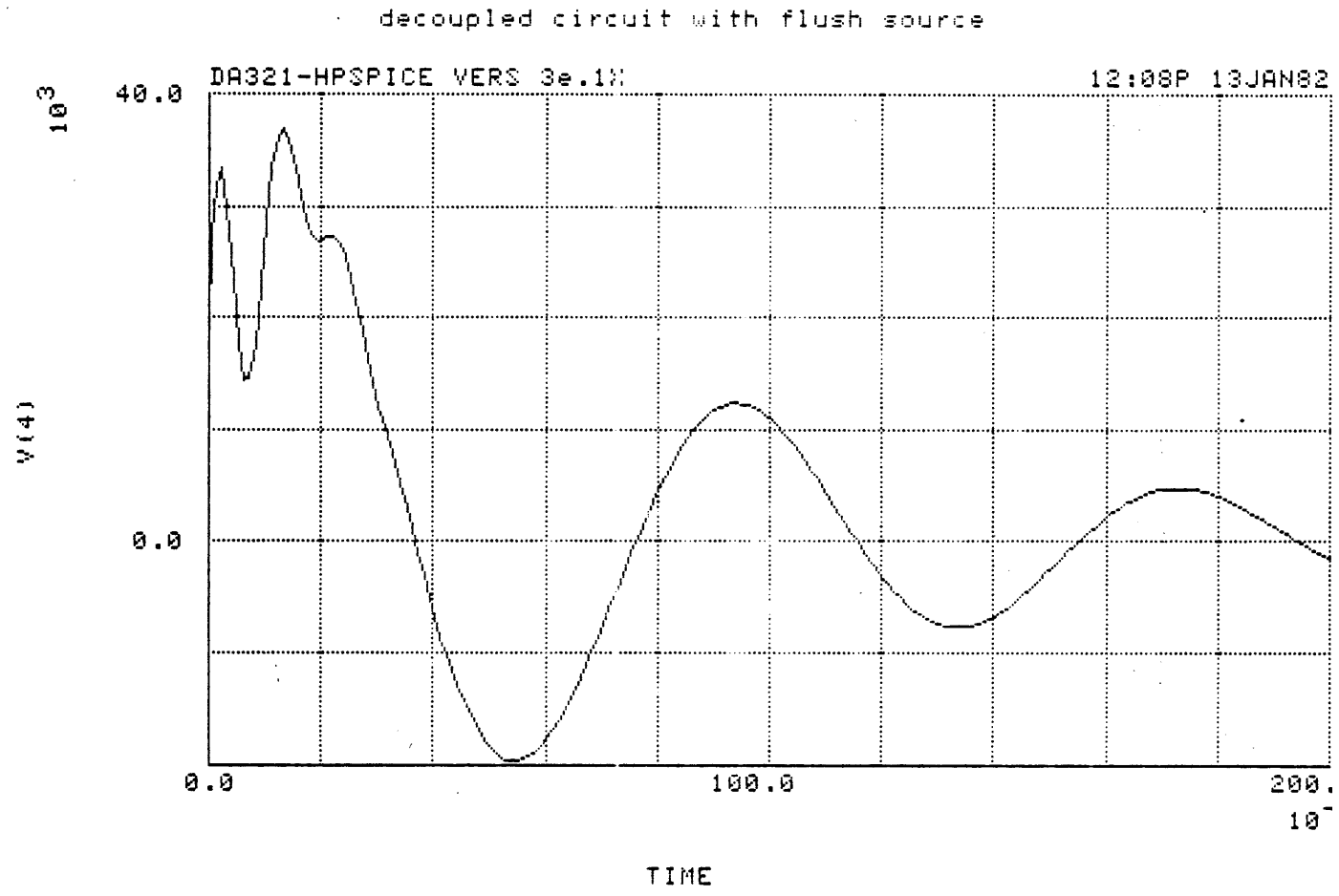

Figure 5-2. Simulated response to fast-flush

5.2 Extraction of Resonant Frequency and Damping from Fast-flush

There is some reason to believe that a good flush source (i.e. one without valve closure artifact) exists or can be designed. What seems to be required is a valve that does not force a bolus of fluid into the fluid column as it closes. However, even if such a device is made available, there are still a number of practical considerations to be considered in attempting to calculate resonant frequency and damping from the flush response.

Foremost among the anticipated difficulties in clinical use of the fast-flush for determining resonant frequency is separating the flush response from the blood pressure waveform. Gardner (1981) has demonstrated the use of the Sorenson in the clinic. The flush valve is released during the diastolic portion of the cardiac cycle where the pressure is changing the most slowly. A recording of the response is then examined. The determination of resonant frequency is relatively easy, but damping requires a careful separation of the superimposed flush and patient waveforms.

We believe that the flush response analysis may be performed by digital computer with high reliability, relieving the hospital personnel of most of the burden of analysis. What is required is some method of patient pressure waveform prediction. This would allow subtraction of the predicted waveform from the superimposed patient and flush waveforms, resulting in a time-domain filtering of the flush response from the combined signal. Statistical

methods of waveform prediction exist, so there is no reason to believe that this computation could not be performed. Other algorithmic devices would have to be designed in order to make the computer calculation reject artifacts, particularly the high-frequency oscillation that we have shown may occur even with an ideal flush source.

5.3 Anticipated Usage and Clinical Acceptability

The issue of clinical acceptance of catheter system measurement/correction devices that require user intervention has been raised (Doherty, 1981). Distortion analysis systems that require no user intervention at all have been described by Doherty and by others (Brower 1975, Jackson et al 1980). The idea of determining and correcting waveform distortion automatically is obviously extremely attractive, but none of the methods described have been shown to reliably estimate distortion over the entire range of catheter systems in use and patient pressure waveforms. Moreover, the central assumption underlying these methods, that the pressure waveform spectrum does not contain local maxima simulating a resonance, is open to some criticism. Whether a method which requires user interaction is acceptable depends in part on how and when the method is intended to be used.

Certainly the calculation of dp/dt is an important part of many catheterization procedures that requires an extremely high-fidelity system. However, a catheter system with poor frequency response will not be suitable for accurate dp/dt

measurements even if it is compensated. Mechanical compensation can only extend the frequency range a limited amount, and inverse filtering methods (Ciccolella 1976) cannot be expected to perform well far beyond resonance where the deviation from second-order response becomes large. Therefore, determination of resonant frequency and damping is probably more important to the physician or technician than elaborate compensation methods when measuring dp/dt. Presently, catheter-tip manometers are the preferred instruments for this measurement, and until fluid-filled systems can reliably achieve flat frequency response to 100 Hz and beyond, this will probably remain the case. Even if debubbled systems become the norm, this will be difficult to achieve given the physics of the fluid column and the need for flexible tubing of reasonable length.

Simple pressure monitoring does not require the large bandwidths of dp/dt measurements, making fluid-filled systems much more attractive. The most common and noticeable effect of low resonant frequency and low damping on the pressure signal is systolic overshoot. If the measurement is being made in a central artery or in the heart, systolic overshoot may falsely indicate a valvular lesion or disease, or high peripheral resistance. In a peripheral artery, the overshoot may falsely trigger pressure alarms. It is with these "suspect" systems that a direct method of determining the system resonant frequency and damping is most needed. In the busy clinical environment, a catheter system that seems to be reproducing the pressure waveform accurately will probably not be tested for adequate frequency response using the

fast-flush or any other technique. However, given a suspicious pressure waveform (damped or resonant-looking), the fast-flush should be able to differentiate between real blood-pressure abnormalities and catheter-induced distortion with high reliability. An occasional flush test does not seem too high a price to pay for higher confidence in the displayed blood pressure waveform.

BIBLIOGRAPHY

1. Brower, R.W., et al: A fully automatic device for compensating for artifacts in conventional catheter-manometer pressure recordings. Biomed. Engng. 10:305-310, 1975.

2. Bruner, J.M.R., et al: Comparison of direct and indirect methods of measuring arterial blood pressure, part 1. Med. Instrum. 15:97-101, 1981.

3. Ciccolella, S.A.: Compensation of fluid-filled catheter response using digital filter techniques. Master's thesis, University of Rhode Island, 1976.

4. Falsetti, H.L., et al: Analysis and correction of pressure wave distortion in fluid-filled catheter systems. Circulation 49:165-172, 1974.

5. Fox, F., et al: Laboratory evaluation of pressure transducer domes containing a diaphragm. Anesth. Analg. 57:67, 1978.

6. Frank, O.: Kritik der elastichen manometer. Zschr. Biol. 44:445-613, 1903.

7. Gabe, I.T.: Pressure measurement in experimental physiology. In Cardiovascular Fluid Dynamics Vol. 1. Edited by Bergel, D.H.. New York: Academic Press, 1972.

8. Gardner, R.M., et al: Catheter-flush system for continuous monitoring of central arterial pulse waveform. J. Appl. Physiol. 29: 911-913, 1970.

9. Gardner, R.M.: Direct blood pressure measurement - dynamic response requirements. Anesthesiology 54:227-236, 1981.

10. Geddes, L.A.: The Direct and Indirect Measurement of Blood Pressure. Chicago: Year Book, 1970.

11. Hansen, A.T.: Pressure measurement in the human organism. Acta Physiol. Scand. 19 (Suppl. 68):1-227, 1949.

12. Hansen, A.T., and Warburg, E.: The theory for elastic liquid-containing membrane manometers. Acta Physiol. Scand. 19 (Suppl. 65):306-332, 1949.

13. Henry, W.L., et al: A calibrator for detecting bubbles in cardiac catheter-manometer systems. J. Appl. Physiol. 23:1007-1009, 1967.

14. Jackson, L.B., Jaron, D., and Wood, S.L.: Compensation of fluid-filled catheter pressure waveforms by linear predictive analysis and digital inverse filtering. Proc. Fifth New Eng. Bioengng. Conf., Apr. 1977.

15. Jager, G.N., Westerhof, N., and Noordergraaf, A.: Oscillatory flow impedance in electrical analog of arterial system. Circ. Research 16:121-133, 1965.

16. Krovetz, L.J., et al: Limitation of correction of frequency dependent artefact in pressure recordings using harmonic analysis. Circulation 50:992-997, 1974.

17. Lambert, E.H., and Wood, E.H.: The use of a resistance wire strain gauge manometer to measure intraarterial pressure. Proc. Soc. Exper. Bio. & Med. 64:186-190, 1947.

18. Lambossy, P.: Oscillations forcees d'un liquide incompressible et visqueux dans un tube rigide et

horizontal. Helv. Phys. Acta 25:371-386, 1952.

19. Lapointe, A.C., and Roberge, F.A.: Mechanical damping of the manometer system used in the pressure gradient technique. IEEE Trans. Biom. Engng. 21:76-77, 1974.

20. Latimer, K.E.: The transmission of sound waves in liquid-filled catheter tubes used for intravascular blood-pressure recording. Med. & Biol. Engng. 6:29-42, 1968.

21. Latimer, K.E., and Latimer, R.D.: Measurements of pressure-wave transmission in liquid-filled tubes used for intravascular blood- pressure recording. Med. & Biol. Engng. 7:143-169, 1969.

22. Li, J.K.-J., van Brummelen, G.W., and Noordergraaf, A.: Fluid- filled blood pressure measurement systems. J. Appl. Physiol. 40:839-843, 1978.

23. McDonald, D.A.: Blood Flow in the Arteries. London: Arnold & Co., 1960.

24. Melbin, J., and Spohr, M.: Evaluation and correction of manometer systems with two degrees of freedom. J. Appl. Physiol. 27:749-755, 1969.

25. Roark, R.J., and Young, W.C.: Formulas for Stress and Strain (p. 104). New York: McGraw-Hill, 1975.

26. Rothe, C.F., and Kim, K.C.: Measuring systolic arterial blood pressure. Critical Care Med. 8:683-689, 1980.

27. Shapiro, G.G, and Krovetz, L.J.: Damped and undamped frequency response of underdamped catheter manometer systems. Am. Heart. J. 80:226-236, 1970.

28. Shinozaki, T., et al: The dynamic responses of liquid- filled catheter systems for direct measurement of blood pressure. Anesthesiology 53:498-504, 1980.

29. Vierhout, R.R.: The response of catheter-manometer systems used for direct pressure recording. Ph.D. thesis, University of Nijmegen, Holland, 1966.

30. Yanof, H.M., et al: A critical study of the response of manometers to forced oscillations. Physics in Med. & Biol. 8:407-422, 1963.

31. Womersley, J.R.: Method for the calculation of velocity, rate of flow and viscous drag in arteries when the pressure gradient is known. J. Physiol. 127:553-563, 1955.

APPENDIX A

Table of Analogous Electrical and Hydraulic Units

Electrical	Hydraulic
Voltage V (V)	Pressure P=F/A (N/m^2 or Pa)
Charge q (coulombs)	Fluid Displacement X=Ax (m^3)
Current I=dq/dt (A)	Fluid Velocity Q=dX/dt=Ax' (m^3/sec)
Power VI (W)	Power PQ (J/sec)
Resistance R=V/I (ohm)	Resistance R=P/Q (Pa-sec/m^3)
Inductance L=V/(dI/dt) (H)	Inertance L=m/A (Pa-sec^2/m^3)
Capacitance C=I/(dV/dt)=q/V (F)	Compliance C=X/P (m^3/Pa)
Kinetic Energy 1/2LI (J)	Kinetic Energy 1/2LQ (J)
Potential Energy 1/2CV (J)	Potential Energy 1/2CP (J)
Resistance/m R'=R/l (ohm/m)	Resistance/m R'=R/l (Pa-sec/m^3)
Inductance/m L'=L/l (H/m)	Inertance/m L'=L/l (Pa-sec^2/m^3)
Capacitance/m C'=C/l (F/m)	Compliance/m C'=C/l (m^3/Pa)

A=cross-sectional area of the tube in m^2
l=length of tubing

APPENDIX B

Calculation of f_n and D From the Step Response

A system is said to be second order if its dynamic response can be described by a second-order differential equation. The second-order equation used to approximate the frequency response of the catheter system is

$$\left[\frac{s^2}{\omega_n^2} + \frac{2Ds}{\omega_n} + 1\right] P_o(t) = P_i(t)$$

where

ω_n = undamped natural frequency (rad/sec)

D = damping ratio (dimensionless)

The step response for an underdamped system (D < 1) is

$$P_0(t) = 1 - \frac{e^{-D\omega_n t}}{\sqrt{1-D^2}} \sin(\sqrt{1-D^2}\omega_n^2 t + \Phi)$$

$$\Phi = \arcsin(\sqrt{1-D^2})$$

We can determine D and ω_n (or $f_n = \frac{\omega_n}{2\pi}$) from the step response by measuring the time between peaks and the ratio of the heights of adjacent peaks. For the typical step response shown below:

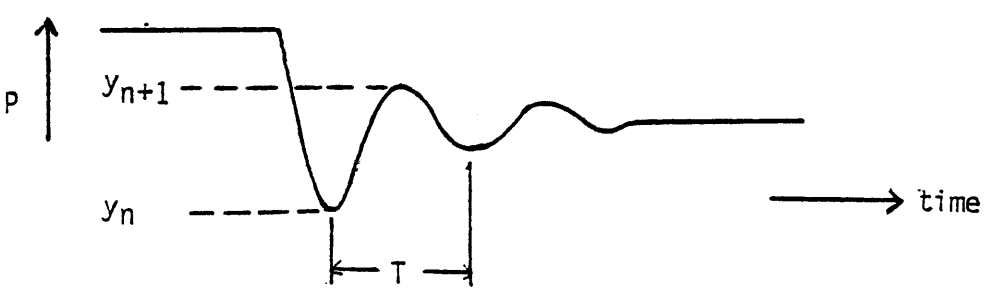

the response reaches a maximum when the sine argument equals $(2n+1)/2\pi$. Solving for tn and the ratio y_n/y_{n+1}, where y_n is the output pressure at time $t=t_n$, we have

$$t_n = \frac{(2n+1)\frac{\pi}{2} - \Phi}{\omega_n\sqrt{1-D^2}}$$

$$\frac{y_n}{y_{n+1}} = e^{(2\pi D/\sqrt{1-D^2})}$$

If we define

$$V = \log_e \frac{y_n}{y_{n+1}}$$

then

$$D = \frac{V}{\sqrt{4\pi^2+V^2}}$$

to solve for f_n, we note the time period between maxima. This yields

$$f_r = 1/T$$

where f_r is the resonant frequency of the system. The natural frequency is simply

$$f_n = f_r/\sqrt{1-D^2} \ .$$